DIPOLAR BOSE-EINSTEIN CONDENSATE IN A CYLINDRICALLY SYMMETRIC TRAP

A THESIS SUBMITTED TO
THE GRADUATE SCHOOL OF ENGINEERING AND SCIENCE
OF BILKENT UNIVERSITY
IN PARTIAL FULFILLMENT OF THE REQUIREMENTS FOR
THE DEGREE OF
MASTER OF SCIENCE
IN
PHYSICS

By
Habib Gültekin
August 2016

DIPOLAR BOSE-EINSTEIN CONDENSATE IN A CYLINDRICALLY SYMMETRIC TRAP

By Habib Gültekin

August 2016

We certify that we have read this thesis and that in our opinion it is fully adequate, in scope and in quality, as a thesis for the degree of Master of Science.

Mehmet Özgür Oktel(Advisor)

Bilal Tanatar

Ali Ulvi Yılmazer

Approved for the Graduate School of Engineering and Science:

Levent Onural
Director of the Graduate School

ABSTRACT

DIPOLAR BOSE-EINSTEIN CONDENSATE IN A CYLINDRICALLY SYMMETRIC TRAP

Habib Gültekin
M.S. in Physics
Advisor: Mehmet Özgür Oktel
August 2016

Bose-Einstein Condensate (BEC) and particularly its stability dynamics has been a subject to many investigations since the first realization of this new condensed state in alkali atoms interacting via short range potential. Short range or contact interactions account for a great number of physical properties ranging from formation of quantum vortices to the superfluid character of cold gases.

In this thesis, dipolar Bose-Einstein condensate, which inherently possess long-range and anisotropic potential for the interaction of the constituent particles, is studied and its stability depending on the geometry of the system is investigated.

The dipolar Bose gas is confined to a cylindrically symmetric harmonic trap and the dipoles within the gas is initially oriented along the symmetry axis of the confining prolate trap. In the condensed state, the condensate is observed to be elongated along harmonic trap symmetry axis as long as the axis corresponds to weak confinement direction. This elongation is understood to be resulting from the energy minimization of the system by adding the dipoles head to tail along the center of the trap, thereby determining the nature of the long-range interaction to be attractive and the condensate is liable to collapse. Below a certain value for the ratio of the dipolar and contact interactions ($\epsilon_{dd} = C_{dd}/3g = 1$), the condensate is stable, while above this value it undergoes collapse. In the opposite case where the trap axis is the strong confinement direction (oblate trap), the elongation occurs perpendicularly to the symmetry axis of the confining trap (with highly oblate geometry) with the energetically most favorable configuration being the alignment of the dipoles side by side implying mostly repulsive interactions in which case the condensate is always stable.

To further understand the effect of the geometry on the stability, the dipoles

are finally oriented at an angle from the trap axis by tuning the external field and elongation direction of the condensate is calculated; stable, metastable and unstable states of the condensate are observed in this new geometry.

Keywords: BEC, Stability, Cold Gases, Contact Interactions, Dipolar Interactions, Cylindrical Trap, Dipoles, Collapse, Elongation.

ÖZET

SİLİNDİRİK SİMETRİK TUZAKTA ÇİFT KUTUPLU BOSE-EINSTEIN YOĞUŞMASI

Habib Gültekin
Fizik, Yüksek Lisans
Tez Danışmanı: Mehmet Özgür Oktel
Ağustos 2016

Bose-Einstein yoğuşması (BEY) ve özellikle yoğuşmanın kararlılık dinamiği, bu yeni yoğunlanmış atomik halin kısa mesafe potensiyelle etkileşen alkali atomlarda ilk gözlenmesinden bu yana, pek çok araştırmanın konusu olmuştur. Kısa mesafe ya da temas etkileşimleri soğuk gazların, kuantum girdabı oluşumundan süperakışkanlığa kadar değişen çok sayıdaki özelliğinden sorumludur.

Bu tezde, bileşen parçacıkların etkileşimi için tabiatı gereği uzun mesafeli ve anizotrop potensiyele sahip olan çift kutuplu Bose-Einstein yoğusması üzerinde çalışılmış ve sistem geometrisine bağlı olan kararlık durumu incelenmiştir.

Çift kutuplu Bose gazı, silindirik simetriye sahip harmonik tuzağa hapsedilmiş ve gazın içinde bulunan dipoller ilk olarak kutupları uzatılmış tuzağın simetri ekseni boyunca yönlendirilmiştir. Yoğunlaşmış durumda, harmonik tuzağın simetri ekseni, zayıf hapsedilme yönüne denk geldiği sürece, yoğuşmanının bu simetri ekseni boyunca uzadığı gözlemlenmiştir. Bu uzamanın, sistemin dipolleri tuzağın merkezi boyunca uç uca ekleyerek enerji minimizasyonu yapmasından kaynaklandığı anlaşılmıştır, böylece uzun mesafeli etkileşimin tabiatı çekici olacak şekilde belirlenmiştir ve yoğuşma çökmeye eğilimlidir. Çift kutuplu ve temas etkileşimleri oranının belli bir değerinin altında ($\epsilon_{dd} = C_{dd}/3g = 1$) yoğuşma kararlıyken, bu değerin üstünde çökmeye uğramaktadır. Tuzak eksenin güçlü hapsedilme yönü olduğu aksi durumdaysa (kutupları yassılaşmış tuzak), yoğuşmanın uzaması tuzağın (büyük ölçüde kutupları yassılaşmş geometriye sahip) simetri eksenine dik olarak gerçekleşmektedir ve enerji açısından en uygun konfigürasyon, yoğuşmanın her zaman kararlı olduğu, çoğunlukla itici etkileşimler anlamına gelen, dipollerin yan yana dizilmesidir.

Geometrinin sistem kararlılığı üzerindeki etkisini daha iyi anlamak için,

dipoller son olarak, dış manyetik alan ayarlanarak, tuzak ekseninden belli bir açıda yönlendirilmiş ve yoğuşmanın uzama yönü hesaplanmıştır; yoğuşmanın bu yeni geometrideki kararlı, yarı kararlı ve kararsız durumları gözlemlenmiştir.

Anahtar sözcükler: BEY, Kararlılık, Soğuk Gazlar, Temas Etkileşimleri, Dipol Etkileşimleri, Silindirik Tuzak, Dipoller, Çökme, Uzama.

To past and future members of my extended family...

Acknowledgement

Writing this thesis does not only reflect the efforts made by me but also it is a product of devotion, common sense, understanding, patience and longing exhibited by a bunch of precious people. This thesis, along with being academic picture of a part of my work in Bilkent University, it is as well an image of my good and bad days with long nights during my graduate study.

First of all, I would like to express my sincere gratitude to my supervisor, M. Özgür Oktel for his guidance and allocating considerable time for one-to-one meetings showing his passion to physics and encouragement of young people to make them further contribute to science, along with that for the systematic approach by being like a friend most of the time, and a serious teacher in the remaing. I learnt many approaches and had the opportunity to carry out applications of what I studied throughout the courses I took; and of course Matlab.

I also learnt a lot from the Prof. Bilal Tanatar both through courses I took from him and via the disussions we made based on physics. Ceyhun Bulutay is special in the sense that he was the first academician I met in department of physics just after the graduate acceptance interview, it was the day I discovered his positivity and orientation ability that leads the graduate students to right paths and motivates them which, I know from my personal experience, is vital. I am grateful to the head of physics department Metin Gürses, with whom we personally knew each other through my webmastership duties, for his mostly professional but in essence fatherly nature. I also very much appreciate the endless support of Oğuz Gülseren and it was really fun to work with our secretary Fatma Gül Akca who was also my collogue in some department works. I am very thankful to my committee member Prof. Ali Ulvi Yılmazer for his valuable contributions.

I would like to thank to my friends in Istanbul for not letting me feel lonely either by visiting at any free time or sending hundreds of messages from Whatsapp group. My friend Hazal Arifoğlu deserves my deepest appreciations for her time-free support. My previous officemates Başak Renklioğlu with her helpful charecter

and Ayşe Ferhan Yeşil with her unique manner has been my closest friends during my graduate study; current office friends Mustafa Kahraman, Ekrem Güldeste and also Yağmur Korkmaz are my colleagues of unending overtime including our coffee breaks which became as ritual of Friday evenings. I am really very pleased to know Mite Mijalkov, Yağmur Yardımcı, Tuğba Andaç, in particular I thank Mite for not being tired of asking to go out for chilling every day. I believe all the friendships I made in Bilkent will persist for years to come.

I particularly convey my special thanks to my family for missing me too much without getting bored during all those years away from home, and being always there for me without need of asking. My extended family has been a joy of living for me of which members are, my parents Fikriye and Hüseyin Gültekin, my brother and best friend Selimcan Gültekin and my aunts like a second mother Yasemin Mantarcı and Nuriye Çuhadar, my cousins like sisters Leyla, Dilek, Elif Çuhadar, my uncles Süleyman Yıldırım, Rahmi Çuhadar, Sabri Mantarcı and the youngest members Doruk Alp Yılmaz and Kaan Erçelebi and my brothers Salih Mantarcı, Murat Yılmaz and Hakan Erçelebi, my *pamuk* grandmother Ayşe Yıldırım and my grandfaher Ali Yıldırım who will always be remembered, and never forgotten.

Contents

List of Figures

Chapter 1

Introduction

Bose Einstein condensation is a consequence of Bose statistics in a dilute gas, where the particle-particle interactions are weak, along with the fact that reducing the temperature below a critical value yields an increase in the thermal de Broglie wavelengths of atoms. Below a point that is fixed by a critical temparature (T_{BEC}), the de Broglie wavelength of atoms exceeds the interparticle separation and wavefunctions of individual atoms start to overlap to form the condensed state. In a Bose-Einstein condensate, macroscopic fraction of atoms share the same single-particle state while rest is distributed over remaining energy states.

Previously (starting from 1924), Bose-Einstein Condensation was thought to be a theoretical limit for an ideal gas of bosons that leads to excessive occupation of the ground state at low temperatures, a phenomenon which was first predicted by Bose [1] and Einstein [2, 3]. The discovery of superfluid helium in 1937 [4, 5], has raised the questions whether a BEC was actually achievable. In 1938, F. London proposed that λ-transition in liquid helium was analogous to Bose-Einstein condensation [6]. However, liquid helium was clearly not an ideal gas and the interatomic interactions were strong on account of the high-density liquid phase. Additionally, fraction of the condensed atoms was really low, i.e. single particle state occupation was reduced due to large interactions. The first realization of

BEC was possible in 1995, using Rb atoms by Cornell & Wieman Group in University of Colorado [7], subsequently using Na atoms in Massachusetts Institute of Technology [8]. The Nobel Prize in physics 2001 was awarded jointly to Eric A. Cornell, Wolfgang Ketterle and Carl E. Wieman "for the achievement of Bose-Einstein condensation in dilute gases of alkali atoms, and for early fundamental studies of the properties of the condensates".

By the realization of the BEC [7–9], a new state of matter, degenerate quantum gases attracted great attention and its properties deeply investigated. Most of the novel properties have been understood to be resulting from the interactions between the particles constituting the gas, other than the geometry (trapped gas) dependent features. In a dilute system of gas, where the average interparticle distance is much larger than the scattering length ($n^{-1/3} \gg a$), short range interactions can be approximated by s-wave part of the collisions characterized by a single parameter: s-wave scattering length a_s [10]. These contact interactions are isotropic and short-range; repulsive for positive values of a and attractive otherwise.

The first experimental observations of BEC in dilute atomic gases were made using alkali atoms, as their atomic structure enabled them to be a perfect candidate for optical cooling. At low temperatures, first several atomic samples that experimentally resulted in Bose-Einstein condensed state were rubidium (^{87}Rb) [7], sodium (^{23}Na) [8] and lithium (^{7}Li) [9]. In the case of lithium, interatomic interactions are attractive and for the first time BEC was observed for a system with negative scattering. These experiments were followed by demonstrations of some other atomic species to form BEC: hydrogen (H) [11], potassium (K) [12], helium (He) [13], cesium (Cs) [14], ytterbium (Yb) [15], strontium (Sr) [16, 17], calcium (Ca) [18]. Long predicted hydrogen condensate was observed through a new probing technique, high resolution spectroscopy. The difference from the alkali atom condensates was that the transition to BEC occurred at relatively higher temperatures and the simplicity of the hydrogen gave rise to better understanding of the interatomic potentials. Helium (metastable helium in the lowest triplet state), on the other hand, is special in terms of both historical reasons that led to exploration of BEC, and due to the fact that ground state of helium

is a liquid phase, therefore it has to be condensed in an excited state. BEC is achieved not only by atomic samples but also by some homonuclear molecules including Rb_2, Cs_2, Li_2 [19, 20], K_2 [21].

Advances in the cooling and trapping of polar molecules have given rise to investigation of the BEC capabilities of the dipolar gases [22]. The first successful experimental realization in this direction was, due to its large magnetic dipole moment of $\mu = 6\mu_B$ (μ_B is the Bohr magneton), the Bose-Einstein condensation of chromium (^{52}Cr) in 2005 with a combination of magneto-optical, magnetic, and optical trapping techniques [23] and with a different all-optical method in 2008 [24]. The chromium condensate allowed the research on the effects of the long range and anisotropic dipole-dipole interaction along with the creation of a degenerate quantum gas with tunable dipolar [25] and contact interactions. Recently, condensates of erbium (^{168}Er) [26] and dysprosium (^{164}Dy) [27] have been observed to show dipolar character with even larger dipole moments of $\mu = 7\mu_B$ and $\mu = 10\mu_B$, respectively.

Indeed, all type of atoms has a magnetic dipole moment, therefore dipolar effects can even be seen, for example, in the condensates of the alkali atoms such as Li and K as demonstrated in references [28, 29]. However, Cr, Er and Dy are the atoms with the highest magnetic dipole moments available and observed to form a Bose-Einstein condensate. Dysprosium is the most magnetic element in nature, and it has been observed in reference [27] that the stability of its condensed state depends on the relative angle between the external magnetic field and the axis of the oblate trap, a phenomenon which is only expected to occur in strongly interacting dipolar gas. Erbium was demonstrated to supply Feshbach resonances at the presence of low magnetic fields which allows it to possess strong dipolar iteractions. Both of Er and Dy introduces the BEC system a novel kind of scattering properties as an outcome of their strongly dipolar nature. Although the dysprosium magnetically strongest atom in the nature, some heteronuclear molecules such as ^{40}K ^{87}Rb [30] and ^{23}Na ^{40}K [31, 32], exhibit a stronger dipolar interaction. Dipolar properties of the homonuclear Rb_2 have also been investigated [33].

Throughout this thesis, we will revise the theoretical concepts of BEC and dBEC with inteactions present and examine the effects of the aforementioned two new properties (anisotropy, long range character) that the dipole-dipole interactions introduce to the system. In a dBEC, we will observe that the stability highly depends on the trap geometry and scattering length in contrast to pure BEC (in the absence of dipolar effects).

Overview

The rest of this thesis is organized as follows: in chapter 2 we introduce theoretical concepts for both BEC and dBEC within a mean-field framework. In chapter 3, we apply these ideas derived, to a problem of harmonically trapped (with cylindrical symmetry) dipolar Bose-Einstein condensate of which dipoles are co-oriented with the weak confining direction and examine the geometrical stabilization. In chapter 4, we improve the problem by adding one more parameter to the system, in which we designate separate directions for dipoles and confinement anisotropy. Finally, in chapter 5 we summarize our findings and give an overview for future work.

Chapter 2

General Review on the Theory of BEC and dBEC in a Weakly Interacting Gas at Zero Temperature

Interparticle interactions play a key role in determining the characteristics of quantum gases. As will be discussed in section 2.2, interactions between particles of weakly interacting Bose gases are governed by s-wave scattering. In this case, interatomic potential is the effective pseudo-potential (2.17) which is, indeed, responsible for a vast variety of physical properties of quantum gases. These properties range from means for superfluidity of the gases to formation of quantum vortices [34, 35].

The fact that interactions have a profound effect in the defining structure of the condensate, has given rise to further investigation on various types of the interaction in order to discover new possible properties. To this end, utilization of the dipole-dipole interaction between particles having permanent electric or magnetic dipole moment, have been suggested [25, 36–46]. This new type of interaction has introduced spectacular features via its anisotropic and long range

character while its contact counterpart is isotropic and short range. The two important features can be categorized into two parts regarding to their effects: new scattering properties and influence on the stability of the condensate. Studies involving ground state properties, optical lattices, expansion dynamics and superfluidity, showing the consequence of dipolar interaction can be found in a series of references [44, 47–52]. Anisotropy and long-range character of dipolar interaction allows one to control interparticle interactions by means of tuning the external field or readjusting the trap anisotropy. In contrast to contact interactions, the sign and strength of the dipolar interaction heavily depend on the trap geometry, therefore stability is affected by the anisotropy of the trap.

In this chapter, we describe the properties of the BEC and dBEC within a theoretical framework. In the process, we employ mean-field (or Hatree) approximation which states that many-body wave function can be written as the symmetrized product of single-particle wave functions. The fact that experimental realization of BEC was a consequence of trapped, dilute and weakly interacting Bose gas, encourages us to understand the properties of the gas in such system. We begin with examining an ideal (non-interacting) Bose gas in harmonic confinement, then turn on the interparticle interactions and observe their effects. We then present an insight for the behaviour and stability of a dipolar trapped condensate depending on the trap symmetry, which will constitute a basis for Chapter 3, where we examine a cylindrically trapped dipolar condensate. The discussion we present here is based on the references [53–57].

2.1 The Ideal Bose Gas in Harmonic Trap

In the absence of the interparticle interactions the Hamiltonian describing the N-particle gas of non-interacting bosons can be written as

$$H = \frac{-\hbar^2}{2m} \sum_{i=1}^{N} \vec{\nabla}_i^2 + \sum_{i=1}^{N} V_{tr}(\vec{r}_i), \tag{2.1}$$

since the the experiments giving rise to the realization of BEC was mostly carried out in harmonic traps, we make use of the following trapping potential

$$V_{tr}(\vec{r}) = \frac{1}{2}m(\omega_x x^2 + \omega_y y^2 + \omega_z z^2). \tag{2.2}$$

The ground state ($T = 0$) wave function of the gas reads, as we deal with the bosons,

$$\Psi(\vec{r}_1, \vec{r}_2..., \vec{r}_N) = \prod_{i=1}^{N} \varphi(\vec{r}_i), \tag{2.3}$$

with $\varphi(\vec{r})$ is the lowest single particle state. This problem is simply quantum mechanics textbook discussion of N identical particles in a harmonic oscillator potential where the energy eigenvalues follow from the summation of single particle eigenvalues; eigenfunctions from the product of the single particle eigenfunctions: Considering isotropic case with $\omega_x = \omega_y = \omega_z = \omega$ for a simple qualitative anlaysis

$$\epsilon_{n_x n_y n_z} = \hbar\omega \left(n_x + n_y + n_z + \frac{3}{2} \right), \qquad \varphi_{000} = \left(\frac{m\omega}{\pi\hbar} \right)^{3/4} e^{-m\omega r^2/2\hbar}. \tag{2.4}$$

Therefore, ground state wave function can be written as, in terms of the lowest single particle state with $n_x = n_y = n_z = 0$,

$$\Psi(\vec{r}_1, \vec{r}_2..., \vec{r}_N) = \left(\frac{m\omega}{\pi\hbar} \right)^{3/4} \prod_{i=1}^{N} e^{-m\omega r_i^2/2\hbar}, \tag{2.5}$$

with oscillator frequency ω and the density distribution is $n(\vec{r}) = N|\varphi_{000}(\vec{r})|^2$. However at a finite temperature, particles will be thermally distributed over energetically higher single particle states and corresponding density distribution is determined by the Bose-Einstein distribution,

$$n_B(\epsilon) = \frac{1}{e^{(\epsilon-\mu)/(k_B T)} - 1}, \tag{2.6}$$

where ϵ is the energy of the state of which occupancy we seek. For the macroscopic occupation of the lowest single particle state, the maximum available value of the chemical potential is given by $\mu_{max} = \epsilon_{min} = \epsilon_{000} = (3/2)\hbar\omega$ which is provided by the Bose-Einstein distribution (2.6) such that

$$n_B(\epsilon_{000}) = \frac{1}{e^{(3\hbar\omega/2 - 3\hbar\omega/2)/(k_B T)} - 1} = 1/(1-1) = \infty \tag{2.7}$$

whereas for even higher values $\mu > \mu_{max}$, occupancy of the lowest single particle state becomes negative, which is nonphysical. Assuming $k_B T \gg \hbar\omega$ we can write the number of particles at higher energy (excited) states with energy ϵ as to be equal to the total number of particles,

$$N_{ex}(T_{BEC}, \mu_{max}) \cong N = \int d\epsilon g(\epsilon) n_B(\epsilon) \tag{2.8}$$

where $g(\epsilon)$ is the density of states, and for the present problem it is

$$g(\epsilon) = \frac{d\theta(\epsilon)}{d\epsilon} = \frac{1}{2\hbar\omega}\left(\frac{\epsilon}{\hbar\omega} - \frac{3}{2}\right)^2, \tag{2.9}$$

where $\theta(\epsilon)$ is the total number of states that have energy less than ϵ, then

$$\begin{aligned} N_{ex} &= \int_{3\hbar\omega/2}^{\infty} d\epsilon \frac{1}{2\hbar\omega}\left(\frac{\epsilon}{\hbar\omega} - \frac{3}{2}\right)^2 \frac{1}{e^{(\epsilon-\mu_{max})/k_B T_{BEC}} - 1} \\ &= \int_{3\hbar\omega/2}^{\infty} d\epsilon \frac{1}{2\hbar\omega}\left(\frac{\epsilon}{\hbar\omega} - \frac{3}{2}\right)^2 \frac{1}{e^{(\epsilon/\hbar\omega-3/2)/(k_B T_{BEC}/\hbar\omega)} - 1}, \end{aligned} \tag{2.10}$$

setting $\tilde{\beta} = \hbar\omega/k_B T_{BEC}$ and making change of variable $x = \tilde{\beta}(\epsilon/\hbar\omega - 3/2)$ we have

$$N_{ex} = \frac{1}{2\tilde{\beta}^3}\int_0^{\infty} dx \frac{x^2}{e^z - 1} = \frac{1}{2\left(\frac{\hbar\omega}{k_B T_{BEC}}\right)^3}\Gamma(3)\zeta(3), \tag{2.11}$$

from which critical temperature for Bose-Einstein condensation follows to be,

$$T_{BEC} = 0.941\left(\frac{\hbar\omega}{k_B}\right) N^{1/3}. \tag{2.12}$$

For the anisotropic case, it is suffice to set the oscillator frequency ω equal to the geometric average $\bar{\omega} = (\omega_x\omega_y\omega_z)^{1/3}$. If we call the total number of particles in the ground state as N_0, the total number of particles N is the sum of number of particles in the ground state and in the excited states, i.e. $N = N_0 + N_{ex}$. The equation (2.12) can also be calculated for temperatures higher than T_{BEC}, in the same manner. The ratio of the two equations gives

$$\frac{N_{ex}}{N} = \left(\frac{T}{T_{BEC}}\right)^3, \tag{2.13}$$

writing N_{ex} in terms of N_0, Eq. (2.13) yields the condensate fraction,

$$\frac{N_0}{N} = 1 - \left(\frac{T}{T_{BEC}}\right)^3. \tag{2.14}$$

2.2 Contact Interactions

The temperatures of interest for the cold gases in terms of interactions between constituent particles introduce a low energy and elastic scattering properties. The most important part of the collision is the two-body collisions (with three or more body collisions being relatively less important) with s-wave channel dominating due to fact that the relevant temperatures are really low and the nature of the gas is typically dilute. More importantly, the interparticle interactions depend only on the parameter scattering length which is given, to first order, by the Born approximation to be

$$a_s = \frac{m}{4\pi\hbar^2}\int d^3 r V(\vec{r}), \tag{2.15}$$

from which an effective concept for the interaction can be derived by writing

$$\frac{4\pi\hbar^2 a_s}{m} = \int d^3 r V_{contact}(\vec{r}) \tag{2.16}$$

and at the positions $\vec{r}$ and $\vec{r'}$, two particles within the gas effectively interacts via

$$V_{contact}(\vec{r}, \vec{r'}) = g\delta(\vec{r} - \vec{r'}), \tag{2.17}$$

where g is the coupling constant for the contact interaction

$$g = \frac{4\pi\hbar^2 a_s}{m}. \tag{2.18}$$

Despite the simple form of the pseudo-potential (2.17), it is the interaction responsible for a vast number of properties of the cold gases which are not observed in its absence. Repulsive and attractive interactions, which are the result of the positive and negative values of the scattering length a_s, has a direct effect on the stability of the Bose gas. In the presence of the repulsive interactions BEC is always stable, whereas attractive interactions give rise to unstable condensate as long as the number of particles N is above a critical value N_c (varies on the details of the system), below which the condensate is in a metastable state with energy having only a local minimum. Contact interactions are well approximated by (2.17) and it is sufficient to utilize it to calculate the energy contribution to the total energy of the condensate, as a result of the particle-particle interactions in short range.

2.3 Mean-Field Approximated Condensed State Theory of Weakly-Interacting Trapped Bosons

In the mean-field regime, many-body wave function for the fully condensed state is obtained by putting all N bosons in the same single particle state $\varphi(\vec{r}_i)$, namely

$$\Psi(\vec{r}_1, \vec{r}_2 ..., \vec{r}_N) = \prod_{i=1}^{N} \varphi(\vec{r}_i), \tag{2.19}$$

and the single particle wave function $\varphi(\vec{r})$ satisfies the following normalization condition

$$\int d^3r |\varphi(\vec{r})|^2 = 1. \tag{2.20}$$

The Hamiltonian describing the Bose-Einstein condensed state can be written as

$$H = \frac{-\hbar^2}{2m} \sum_{i=1}^{N} \vec{\nabla}_i^2 + \sum_{i=1}^{N} V_{tr}(\vec{r}_i) + \sum_{i<j} V_{ij}(r_i, r_j), \tag{2.21}$$

where N is the total number of particles within the cloud, V_{ij} is the effective particle-particle interaction (2.17), $\hbar$ is the reduced Planck's constant, m is the mass of a single particle and V_{tr} is the external trapping potential for a single particle. The energy of the N-particle state is given by the expectation value of the Hamiltonian (2.21) in the state (2.19)

$$E = -\frac{\hbar^2}{2m} N \int d^3r \varphi^*(\vec{r}) \nabla^2 \varphi(\vec{r}) + N \int d^3r \varphi^*(\vec{r}) V(\vec{r}) \varphi(\vec{r})$$

$$+ \binom{N}{2} \underbrace{g \int d^3r \int d^3r' |\varphi(\vec{r})|^2 |\varphi(\vec{r'})|^2 \delta(\vec{r} - \vec{r'})}_{E_{ij}^{int}} \tag{2.22}$$

where in the last term, we have multiplied interaction energy E_{ij}^{int} between any two particles sharing the same single particle state $\varphi(\vec{r})$ with total number of pairs which is given by 2-combinations of N. We next arrange terms by carrying out the delta function integral in the last term and make use of the identity for the first term

$$-\varphi^*(\vec{r}) \nabla^2 \varphi(\vec{r}) = |\nabla \varphi(\vec{r})|^2 + \vec{\nabla} \cdot (\varphi^*(\vec{r}) \nabla \varphi(\vec{r})) \tag{2.23}$$

where the second term in the right side of the equality (2.23) produces surface term (by virtue of Green's theorem) having zero contribution to the energy. Therefore, the energy (2.22) can be written as,

$$E = \int d^3r \left[\frac{\hbar^2}{2m} N|\nabla\varphi(\vec{r})|^2 + NV(\vec{r})|\varphi(\vec{r})|^2 + \frac{N(N-1)}{2} g|\varphi(\vec{r})|^4 \right]. \tag{2.24}$$

The wave function $\psi(\vec{r})$ of the condensed state can be defined in terms of single particle state $\varphi(\vec{r})$ ($\sim 1/V^{1/2}$) as follows

$$\psi(\vec{r}) = N^{1/2}\varphi(\vec{r}), \tag{2.25}$$

such that the density of the particles ($\sim N/V$ where V is the volume of the system) is given by $n(\vec{r}) = N|\phi(\vec{r})|^2 = |\psi(\vec{r})|^2$ and the normalization condition for this condensed state becomes

$$\int d^3r|\psi(\vec{r})|^2 = N \underbrace{\int d^3r|\varphi(\vec{r})|^2}_{1} = N. \tag{2.26}$$

In terms of the condensed state (2.25), the energy functional (2.24) becomes

$$E = \int d^3r \left[\frac{\hbar^2}{2m}|\nabla\psi(\vec{r})|^2 + V(\vec{r})|\psi(\vec{r})|^2 + \frac{g}{2}|\psi(\vec{r})|^4 - \frac{1}{N} g|\psi(\vec{r})|^4 \right], \tag{2.27}$$

under the assumption that $N \gg 1$, which is valid for realistic BEC systems, leaves the term proportional to $1/N$ negligible. As a result, The energy of the condensate reads

$$E = \int d^3r \left[\frac{\hbar^2}{2m}|\nabla\psi(\vec{r})|^2 + V(\vec{r})|\psi(\vec{r})|^2 + \frac{g}{2}|\psi(\vec{r})|^4 \right]. \tag{2.28}$$

The ψ that minimizes the energy is found by employing method of Lagrange multipliers with the constraint that total number of particles is constant. We have

$$\psi^* \to \psi^* + \delta\psi^*, \qquad \frac{\delta(E+\mu N)}{\delta\psi^*} = 0, \tag{2.29}$$

therefore

$$(E-\mu N)+\delta(E-\mu N)=\int d^3r\left[\frac{\hbar^2}{2m}\vec{\nabla}(\psi^*+\delta\psi^*)\cdot\nabla(\psi)+V(\vec{r})(\psi^*+\delta\psi^*)\psi\right.$$
$$\left.+\frac{g}{2}(\psi^*+\delta\psi^*)(\psi^*+\delta\psi^*)\psi\psi-\mu\psi^*\psi-\mu\delta\psi^*\psi\right]$$
$$=\underbrace{\int d^3r\left[\frac{\hbar^2}{2m}|\nabla\psi(\vec{r})|^2+V(\vec{r})|\psi(\vec{r})|^2+\frac{g}{2}|\psi(\vec{r})|^4-\mu|\psi(\vec{r})|^2\right]}_{(E-\mu N)}$$
$$+\underbrace{\int d^3r\delta\psi^*\left[\frac{-\hbar^2}{2m}\nabla^2\psi+V(\vec{r})\psi+g|\psi|^2\psi-\mu\psi\right]}_{\delta(E-\mu N)} \tag{2.30}$$

then variation of $E-\mu N$ with respect to $\psi^*(\vec{r})$ becomes

$$\frac{\delta(E-\mu N)}{\delta\psi^*}=\int d^3r\left[\frac{-\hbar^2}{2m}\nabla^2\psi+V(\vec{r})\psi+g|\psi|^2\psi-\mu\psi\right]=0, \tag{2.31}$$

which gives the time-independent Gross-Pitaevskii equation

$$\frac{-\hbar^2}{2m}\nabla^2\psi(\vec{r})+V(\vec{r})\psi(\vec{r})+g|\psi(\vec{r})|^2\psi(\vec{r})=\mu\psi(\vec{r}). \tag{2.32}$$

The Gross-Pitaevskii equation is in the form of nonlinear Schrodinger equation, due to the nonlinear contact interaction term $g|\psi(\vec{r})|^2\psi(\vec{r})$. The eigenvalue is the chemical potential μ, instead of the energy of a single particle. The Gross-Pitaevskii equation describes the properties of non-uniform dilute and weakly interacting Bose gas at zero temperature. We can obtain solutions of a particular system either by exactly or numerically solving the Gross-Pitaevskii equation (2.32), alternatively we can utilize a variational approach which requires the substitution of the trial function that describes the most general ground state of the system, into the energy functional (2.28) to be minimized for finding the optimal values of the variational parameters.

2.4 Thomas-Fermi Approximation

Let us begin this section with analyzing a problem where a weakly-interacting BEC trapped in an isotropic harmonic oscillator potential

$$V(x,y,z) = \frac{1}{2}m\omega_0^2(x^2+y^2+z^2), \tag{2.33}$$

utilizing a variational approach based on the following Gaussian ansatz

$$\psi(x,y,z) = \sqrt{\frac{N}{\pi^{3/2}R^3}}e^{-(x^2+y^2+z^2)/2R^2}. \tag{2.34}$$

with R being the radius of the condensate that we treat as the variational parameter. Substituting this trial wave function (2.34) into Eq. (2.28) gives the energy expression

$$E(R) = \frac{N\hbar^2}{4m}\frac{1}{R^2} + \frac{Nm\omega_0^2}{4}R^2 + \frac{g}{4\sqrt{2}\pi^{3/2}}\frac{N^2}{R^3}. \tag{2.35}$$

Minimizing E with respect to variational parameter R yields the equation

$$R^5 - l^4R - \frac{3\sqrt{2}}{\sqrt{\pi}}aNl^4 = 0. \tag{2.36}$$

where $l = \sqrt{\hbar/m\omega_0}$ is the oscillator length scale, a is the scattering length, N the number of particles within the cloud. Scaling the variational parameter R with l such that $\tilde{R} = R/l$ we have

$$\tilde{R}^5 - \tilde{R} - \frac{3\sqrt{2}}{\sqrt{\pi}}\left(\frac{Na}{l}\right) = 0. \tag{2.37}$$

As can be seen from Fig. 2.1 that for $(Na/l) >> 1$, the contribution to Eq. (2.37) from the kinetic energy term which is proportional to $\sim R$, can be neglected.

In general, when the number of particles in the cloud is sufficiently large, which is determined by the condition $(Na/l) >> 1$, the kinetic energy is small compared to potential energy and interaction energy. Therefore, solutions obtained by neglecting kinetic energy term is within a good approximation. Such solutions are represented by the Thomas-Fermi wave function which is obtained by Gross-Pitaevskii equation (2.32) with the kinetic energy term omitted, namely

$$V(\vec{r})\psi(\vec{r}) + g|\psi(\vec{r})|^2\psi(\vec{r}) = \mu\psi(\vec{r}), \tag{2.38}$$

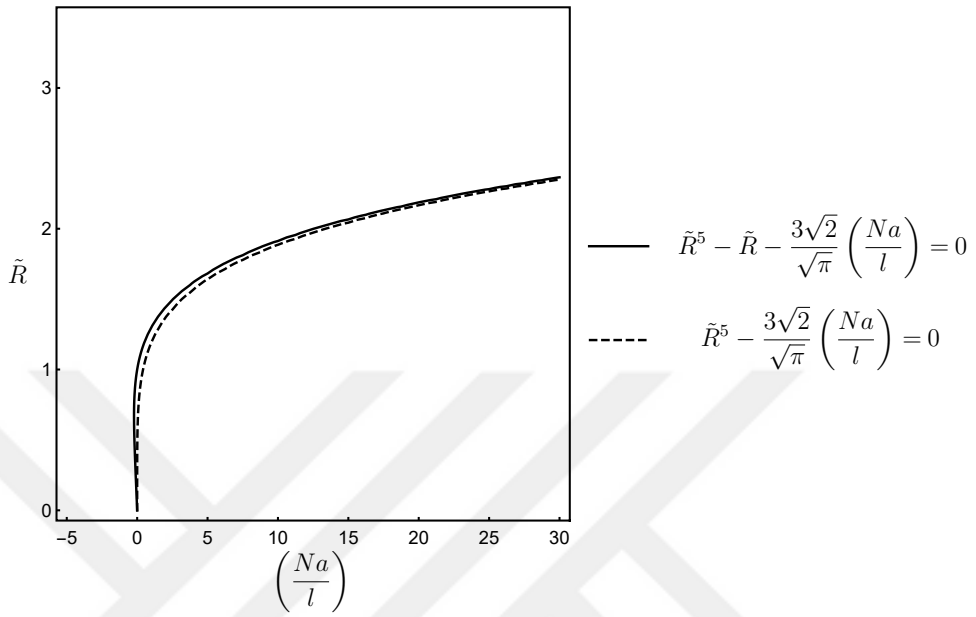

Figure 2.1: Plot of the Eq. (2.37) shows that contribution to the energy from the kinetic energy term becomes less important as the parameter Na/l is increased.

the TF wave function generated by this GP equation is

$$\psi(\vec{r}) = \sqrt{\frac{\mu - V(\vec{r})}{g}}, \tag{2.39}$$

subjected to the conditions $n(\vec{r}) = |\psi(\vec{r})|^2 \geq 0$, therefore at the surface ($n(\vec{r}) = 0$) of the cloud $V(\vec{r})|_{r=R} = \mu$, where R is the radius of the condensate, μ is the chemical potential and $r = \sqrt{x^2 + y^2 + z^2}$. As an example, in the case of spherically symmetric harmonic potential (2.33), the TF wave function reads

$$\psi(r) = \sqrt{\frac{m\omega_0^2}{2g}(R^2 - r^2)}, \tag{2.40}$$

subjected to the normalization condition (2.26),

$$\begin{aligned} N &= \int d^3r \frac{m\omega_0 R^2}{2g}\left(1 - \frac{r^2}{R^2}\right) \\ &= \frac{m\omega_0 R^2}{2g} \underbrace{\int_0^{\pi} \sin\theta d\theta}_{2} \underbrace{\int_0^{2\pi} d\phi}_{2\pi} \underbrace{\int_0^{R} dr r^2 \left(1 - \frac{r^2}{R^2}\right)}_{2R^3/15} \\ &= \frac{4\pi m\omega_0^2}{15g} R^5, \end{aligned} \tag{2.41}$$

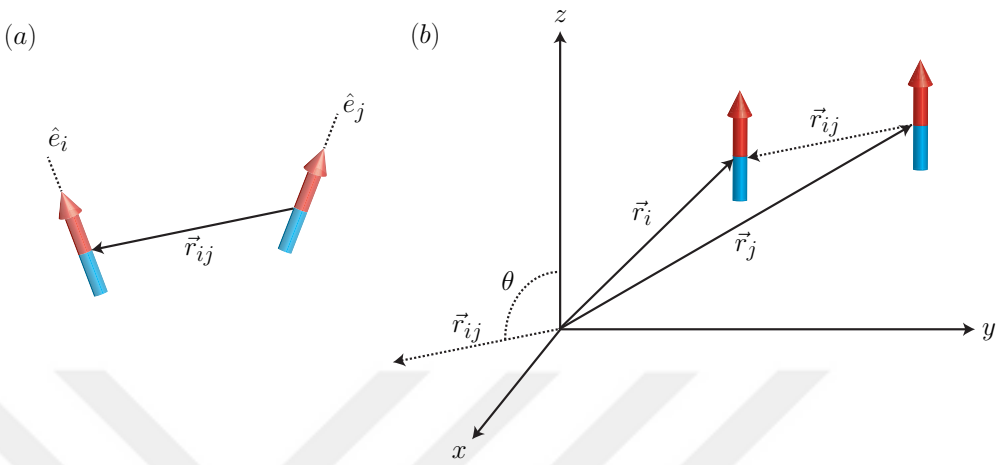

Figure 2.2: Schematic representation of dipole-dipole interaction in the case of dipoles are aligned.

which gives the relation between the radius R of the condensate and the number of particles N it contains,

$$R = \left(\frac{15g}{4\pi m\omega_0^2}N\right)^{1/5}. \tag{2.42}$$

2.5 Dipole-Dipole Interactions

In the beginning, we inspect the long range dipolar potential through which particles having dipole moment interact. For any two particles with dipole moments along $\hat{e}_i$ and $\hat{e}_j$ respectively, the dipole-dipole potential is

$$V_{dd}(r_{ij}) = g_{dd}\frac{(\hat{e}_i\hat{e}_j)r_{ij}^2 - 3(\hat{e}_i\vec{r}_{ij})(\hat{e}_j\vec{r}_{ij})}{r_{ij}^5} = g_{dd}\frac{\delta_{ij} - 3\hat{e}_i\hat{e}_j}{r_{ij}^3}, \tag{2.43}$$

where $r_{ij} = |\vec{r}_i - \vec{r}_j|$ is the relative position of ith and jth particles; g_{dd} is the long range interaction strength. Particles with magnetic dipole moment μ have (using SI) $g_{dd} = \mu_0\mu^2/4\pi$; whereas particles with electric dipole moment d have $g_{dd} = d^2/4\pi\epsilon_0$ and we generalize this concept to include both types of the moments: $g_{dd} = C_{dd}/4\pi$, where C_{dd} is referred to as dipolar coupling constant in literature and includes the information of the dipolar interaction to be either magnetic or electric.

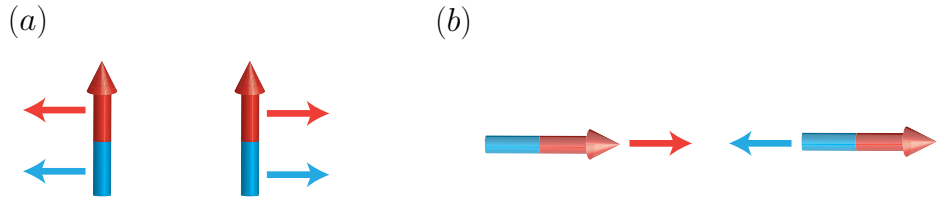

Figure 2.3: A configuration of dipoles, (a) two polarized dipoles placed side by side repel each other; (b) two polarized dipoles positioned head to tail attract one another.

Assuming that the dipoles are polarized along $\hat{z}$ direction, the situation which we will use most, the dipole-dipole potential reads

$$V_{dd}(r_{ij}) = \frac{C_{dd}}{4\pi}\frac{(\hat{z}.\hat{z})r_{ij}^2 - 3(\hat{z}.\vec{r}_{ij})^2}{r_{ij}^5} = \frac{C_{dd}}{4\pi}\frac{1-3(\hat{z}.\vec{r}_{ij})^2}{r_{ij}^5} = \frac{C_{dd}}{4\pi}\frac{1-3\cos^2\theta}{r_{ij}^3}, \quad (2.44)$$

where θ is the angle between polarization direction $\hat{z}$ and the relative position r_{ij}.

One of the most important property of dipolar interactions relevant to this thesis is its *anisotropy*, which is is due to $\cos^2\theta$ term in Eq. (2.44). In the two limiting cases $\theta = 0$ and $\theta = \pi/2$, the $1-3\cos^2\theta$ factor reads -2 and 1, respectively. Consequently, dipoles placed side by side ($\theta = \pi/2$) repel each other, while dipoles positioned head to tail ($\theta = 0$) attract one another with the twice strength of the preceding case (Fig. 2.3). At the special value $\theta = 54.7$, called magic angle, $V_{dd}(r_{ij}) = 0$. The above discussion suggest that the behaviour of the dipolar condensate depends on the geometry of the system, so that the condensate could possess either attractive or repulsive interparticle interactions depending on the relative alignment of the dipoles characterized by the angle θ, the dipolar effects could even vanish.

Another major property is the *long range* character of the dipolar interaction due to factor $1/r^3$ whereas in the case of short range contact interactions (e.g. van der Waals) the interaction typically proportional to $-1/r^6$. The dipolar interaction also introduces the system a new set of *scattering properties*.

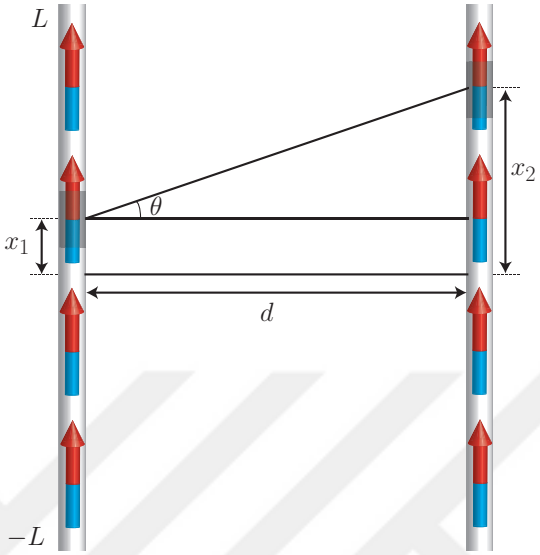

Figure 2.4: Sketch of the example where two lines of dipoles are placed parallel

It is instructive for later purposes to visualize the dipolar interaction by considering the interaction between two line of dipoles. The corresponding configuration is represented in Fig. 2.4. Since the $\cos\theta$ and the relative distance r_{12} of the dipoles can be respectively written from the figure as

$$\cos\theta = \frac{(x_2 - x_1)^2}{[(x_2 - x_1)^2 + d^2]}, \qquad r_{12} = \left[(x_2 - x_1) + d^2\right]^{3/2} \tag{2.45}$$

where the dipole-dipole interaction is

$$V_{dd}(r_{12}) = \frac{C_{dd}}{4\pi}\frac{1 - 3\cos^2\theta}{r_{12}^3}. \tag{2.46}$$

As a result the dipolar interaction (2.44) for this problem reads

$$V_{dd}(r_{12}) = \frac{C_{dd}}{4\pi}\frac{1 - 3\cos^2\theta}{r_{12}^3} = \frac{1 - 3(x_2 - x_1)^2/[(x_2 - x_1)^2 + d^2]}{[(x_2 - x_1) + d^2]^{3/2}}$$

$$= \frac{d^2 - 2(x_2 - x_1)^2}{[(x_2 - x_1) + d^2]^{5/2}} \tag{2.47}$$

Total interaction energy is calculated as in the following way

$$\begin{aligned} U_{12} &= \int dx_1 dx_2 n_1(x_1) n_2(x_2) V_{dd}(x_1 - x_2) \\ &= \lambda_0^2 \int_{-L}^{L} dx_1 \int_{-L}^{L} dx_2 \frac{d^2 - 2(x_2 - x_1)^2}{\left[(x_2 - x_1) + d^2\right]^{5/2}} \\ &= \lambda_0^2 \left[\frac{2}{d} - \frac{1}{\sqrt{4L^2 + d^2}}\right]. \end{aligned} \tag{2.48}$$

2.6 Characteristics of the Dipolar Bose Gas

The total interaction in the case of a dipolar gas is given by the combination of contact and long range interactions

$$V_{int} = \frac{4\pi\hbar^2 a_s}{m}\delta(\vec{r} - \vec{r'}) + \frac{C_{dd}}{4\pi}\frac{1 - 3\cos^2\theta}{|\vec{r} - \vec{r'}|^3}, \tag{2.49}$$

with this interaction potential, the stationary GP equation (2.32) for a dipolar gas reads

$$\begin{aligned} &\frac{-\hbar^2}{2m}\nabla^2\psi(\vec{r}) + V(\vec{r})\psi(\vec{r}) \\ &\qquad + \left(g|\psi(\vec{r})|^2 + \frac{C_{dd}}{4\pi}\int d^3r' |\psi(\vec{r'})|^2 \frac{1 - 3\cos^2\theta}{|\vec{r} - \vec{r'}|^3}\right)\psi(\vec{r}) = \mu\psi(\vec{r}). \end{aligned} \tag{2.50}$$

In order to find stable solutions for the condensate wave function, one needs to solve the time-independent Gross-Pitaevskii equation (2.50). However, this equation cannot be solved analytically, even for a spherically symmetric trap with $\omega_x = \omega_y = \omega_z$. For this reason, numerical, variational and approximate methods are performed to investigate the behaviour of solutions to Eq .(2.50). In this thesis, we mainly make use of the variational approach with the Gaussian ansatz and the energy functional

$$\begin{aligned} E = \int d^3r \Bigg[&\frac{\hbar^2}{2m}|\overrightarrow{\nabla}\psi|^2 + V_{tr}(\rho, z)|\psi|^2 \\ &+ \frac{g}{2}|\psi|^4 + \frac{C_{dd}}{8\pi}|\psi|^2 \int d^3r' |\psi(r')|^2 \frac{1 - 3\cos^2\theta}{|\vec{r} - \vec{r'}|^3}\Bigg]. \end{aligned} \tag{2.51}$$

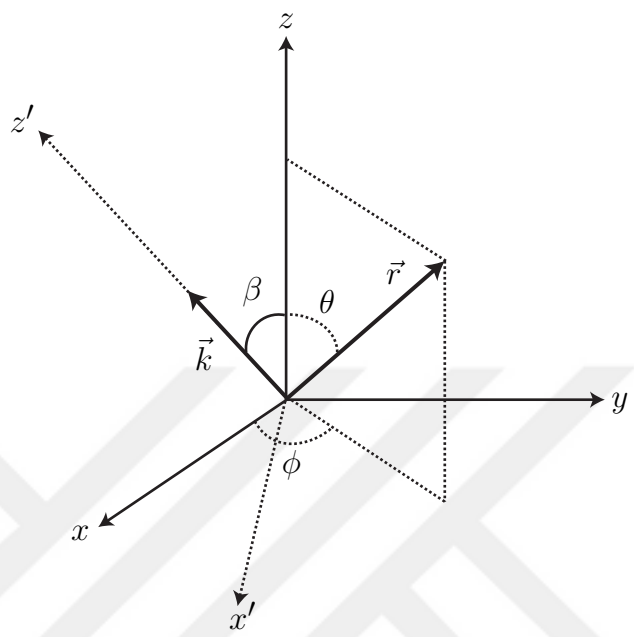

Figure 2.5: Sketch of quantities entering the Fourier transform calculation of V_{dd}.

2.7 Fourier transform of the dipole-dipole interaction

In the analysis of trapped dipolar condensates, Fourier transform of the dipole-dipole interactions simplifies the manipulation of the integral appearing in the long-range interaction term of the energy. In this section, it is intended to derive this transform. The dipolar potential can be rewritten as

$$V(\vec{r}) = \frac{C_{dd}}{4\pi}\frac{1-3\cos^2\theta}{r^3} = \frac{C_{dd}}{4\pi}\frac{1-3z^2/r^2}{r^3}, \tag{2.52}$$

then, the Fourier transform of this potential is

$$\begin{aligned}\tilde{V}(\vec{k}) &= \frac{C_{dd}}{4\pi}\int d^3r V(\vec{r}) e^{-i\vec{k}.\vec{r}} \\ &= \frac{C_{dd}}{4\pi}\int dxdydz \frac{1-3\frac{z^2}{r^2}}{r^3} e^{-i|\vec{k}|(z\cos\beta + x\sin\beta)}\end{aligned} \tag{2.53}$$

where $\vec{r} = x\hat{x} + y\hat{y} + z\hat{z}$, $\vec{k} = |\vec{k}|\cos\beta\hat{x} + |\vec{k}|\cos\beta\hat{z}$

$$\begin{aligned}\tilde{V}(\vec{k}) &= \frac{C_{dd}}{4\pi}\int dxdydz\frac{1-\frac{3}{r^2}(cos\beta z' - \sin\beta x')^2}{r^3}e^{-i|\vec{k}|z'} \\ &= \frac{C_{dd}}{4\pi}\int_0^\infty dr\int_0^{2\pi} d\phi\int_0^\pi d(\cos\theta) \\ &\times \frac{1-3(\cos\beta\cos\theta - \sin\beta\sin\theta\cos\phi)^2}{r}e^{-i|\vec{k}|r\cos\theta}\end{aligned} \tag{2.54}$$

change of variable $u = \cos\theta$ yields

$$\begin{aligned}\tilde{V}(\vec{k}) =& 2\pi\int_0^\infty dr\int_{-1}^1 du\frac{(1-3\cos^2\beta u^2 - \frac{3}{2}\sin^2\beta(1-u^2))}{r}e^{-i|\vec{k}|ru} \\ =& \pi\frac{C_{dd}}{4\pi}(3cos^2\beta - 1)\int_0^\infty d(|\vec{k}|r)\int_{-1}^1 du\frac{(1-3u^2)}{|\vec{k}|r}e^{-i|\vec{k}|ru}\end{aligned} \tag{2.55}$$

performing change of variable $z = |\vec{k}|r$

$$\begin{aligned}\tilde{V}(\vec{k}) &= \frac{C_{dd}}{4}(3cos^2\beta - 1)\int_0^\infty dz\int_{-1}^1 du\frac{(1-3u^2)}{z}e^{-izu} \\ &= C_{dd}(3cos^2\beta - 1)\int_a^\infty dz\left(-\frac{\sin z}{z^2} - 3\frac{\cos z}{z^3} + 3\frac{\sin z}{z^4}\right)\end{aligned} \tag{2.56}$$

where a is cut-off, carrying out the integral over z we have

$$\tilde{V}(\vec{k}) = C_{dd}(3\cos^2\beta - 1)\left(-\frac{\cos a}{a^2} + \frac{\sin a}{a^3}\right) \tag{2.57}$$

with

$$\lim_{a\to 0}\left(-\frac{\cos a}{a^2} + \frac{\sin a}{a^3}\right) = \frac{1}{3},$$

the Fourier transform of the dipolar potential becomes

$$\tilde{V}(\vec{k}) = C_{dd}\left(\cos^2\beta - \frac{1}{3}\right), \tag{2.58}$$

where it follows from Fig.2.5 that $\cos\beta = k_z/k$.

Chapter 3

Dipole Orientation Along the Trap Symmetry Axis

In this chapter, we examine a BEC with dipolar interactions in a cylindrical harmonic trap $V_{tr}(\rho, z) = m\omega_{\perp}^2 \left(\rho^2 + \lambda^2 z^2\right)/2$. We confine the cloud less strongly in the alignment direction of dipoles ($\lambda = \omega_z/\omega_{\perp} < 1$) which is taken to be z. The results we present here is the reproduction of the discussions made in papers [36, 48, 58–61]. On account of the dipolar interactions, we expect the dipoles to reconfigure their location in favor of the minimum energy. However, as the trap symmetry suggests, the condensate should elongate along the weak direction of the trap, up to a limiting ratio between the strengths of contact and dipolar interactions. Since the dipoles will form a head to tail configuration, the dipolar part of the interaction is attractive while contact interaction is repulsive. As soon as the overall strength of the dipolar interaction exceeds the contact one, the condensate will start to collapse. For this reason, the balance between the two kinds of interactions plays a profound role in the stability of the dipolar gas with the present cylindrically symmetry.

The trap geometry also drastically affects the stability of the dipolar Bose Einstein condensate, this is due to anisotropic character of the dipolar interaction. For the trap symmetry ($\lambda = \omega_z/\omega_{\perp} > 1$), the dipole-dipole interaction is mostly

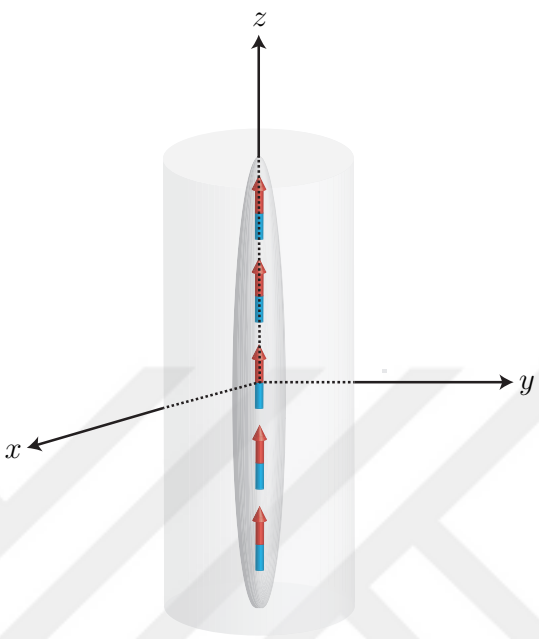

Figure 3.1: The schematic representation of the present problem, with cigar-shaped condensate and cylindrically symmetric trap, where the dipoles are aligned in the weak confinement direction z of the trap.

repulsive and the condensate could be either stable or unstable depending on the strength and the sign of the contact interactions. We continue this section by first deriving energy expression for the described system (Sec. 3.1), then put the equations in dimensionless form (Sec. 3.2) for both visualization purposes (Fig. 3.4) and to obtain graphical solution of the transcendental equation appear when minimizing the energy expression (Sec. 3.3). In Sec. 3.4, we investigate the stability of the condensate by graphically solving this transcendental equation and in Sec. 3.5 we connect our findings to the case of Thomas-Fermi approximated dipolar Bose gas. In the last section (Sec. 3.6) of this chapter we analyze, with a straightforward example, the facts behind the elongation of the condensate.

3.1 Obtaining the Energy by Variational Method

We invoke a variational approach to determine the energy of the cloud and to do that, we utilize the following Gaussian trial function which is normalized to N,

due to the fact that, in the absence of particle-particle interactions, ground state wave function is a Gaussian

$$\psi(x,y,z) = \sqrt{\frac{N}{\pi^{3/2}R_\perp^2 R_z}} e^{-\frac{x^2+y^2}{2R_\perp^2}-\frac{z^2}{2R_z^2}} \tag{3.1}$$

where $R_\perp$, R_z are variational parameters. Energy functional for the dipolar gas reads

$$E[\psi] = \int d^3r \left[\frac{\hbar^2}{2m}|\vec{\nabla}\psi|^2 + V_{tr}(\rho,z)|\psi|^2 + \frac{g}{2}|\psi|^4\right] + \frac{1}{2}\int d^3r|\psi|^2\Phi_{dd}(\vec{r}), \tag{3.2}$$

where

$$\Phi_{dd}(\vec{r}) = \int d^3r' n(r')V_{dd}(r-r') \tag{3.3}$$

is the the mean field potential due to dipole-dipole interactions, $V_{tr}(\rho,z)$ is the external potential due to trap and we set it to have cylindrical symmetry to have cigar-shaped cloud as the final stable configuration, $n(r') = |\psi(r')|^2$ is the density of the condensate, therefore external potential is

$$V_{tr}(\rho,z) = \frac{1}{2}m\omega_\perp^2(x^2+y^2) + \frac{1}{2}m\omega_z^2 z^2. \tag{3.4}$$

We obtain expression for energy as a function of condensate radii, by inserting the Gaussian ansatz into the energy functional (3.2). Energy of the system can be written as sum of each contribution

$$E = E_{kin} + E_{pot} + E_1^{int} + E_2^{int}, \tag{3.5}$$

We now depict the calculation steps of each term in the following subsections.

3.1.1 Kinetic Energy Term

The kinetic energy defined by the first term in Eq. (3.2), is also called as the quantum pressure which pushes the atoms outward and flattens the central density by extending the condensate radius

$$E_{kin} = \int d^3r \frac{\hbar^2}{2m}|\vec{\nabla}\psi|^2, \tag{3.6}$$

where the absolute square of the gradient of the wave function in cylindrical coordinates can be calculated as the following

$$|\overrightarrow{\nabla}\psi|^2 = \left|\left(\hat{\rho}\frac{\partial}{\partial\rho} + \hat{z}\frac{\partial}{\partial z}\right)\psi\right|^2$$

$$= \left(\hat{\rho}\frac{\partial}{\partial\rho}\psi + \hat{z}\frac{\partial}{\partial z}\psi\right)\cdot\left(\hat{\rho}\frac{\partial}{\partial\rho}\psi + \hat{z}\frac{\partial}{\partial z}\psi\right)$$

$$= \left(\frac{\partial}{\partial\rho}\psi\right)^2 + \left(\frac{\partial}{\partial z}\psi\right)^2, \tag{3.7}$$

and derivatives follow as

$$\frac{\partial}{\partial\rho}\psi = \frac{\partial}{\partial\rho}\left(\sqrt{\frac{N}{\pi^{3/2}R_\perp^2 R_z}}e^{-\frac{\rho}{2R_\perp^2}-\frac{z^2}{2R_z^2}}\right) = -\frac{\rho}{R_\perp^2}\psi$$
$$\frac{\partial}{\partial z}\psi = \frac{\partial}{\partial z}\left(\sqrt{\frac{N}{\pi^{3/2}R_\perp^2 R_z}}e^{-\frac{\rho}{2R_\perp^2}-\frac{z^2}{2R_z^2}}\right) = -\frac{z}{R_z^2}\psi \tag{3.8}$$

substituting Eq. (3.7) and Eq. (3.8) into equation Eq. (3.6) we get

$$E_{kin} = \frac{\hbar^2}{2m}\int_0^\infty 2\pi\rho\int_{-\infty}^\infty dz\frac{\rho^2}{R_\perp^4}|\psi|^2 + \frac{\hbar^2}{2m}\int_0^\infty 2\pi\rho\int_{-\infty}^\infty dz\frac{z^2}{R_\perp^4}|\psi|^2$$

where ψ is given in Eq. (3.1)

$$E_{kin} = \frac{\pi\hbar^2}{m}\left(\frac{N}{\pi^{3/2}R_\perp^2 R_z}\right)^2\Bigg[\frac{1}{R_\perp^4}\underbrace{\int_0^\infty d\rho\rho^3 e^{-\frac{\rho^2}{R_\perp^2}}}_{R_\perp^4/2}\underbrace{\int_{-\infty}^\infty dz e^{-\frac{z^2}{R_z^2}}}_{R_z\sqrt{\pi}}$$
$$+\frac{1}{R_\perp^4}\underbrace{\int_0^\infty d\rho\rho e^{-\frac{\rho^2}{R_\perp^2}}}_{R_\perp^2/2}\underbrace{\int_{-\infty}^\infty dz z^2 e^{-\frac{z^2}{R_z^2}}}_{R_z^3\sqrt{\pi}/2}\Bigg], \tag{3.9}$$

arranging the terms to conclude

$$E_{kin} = \frac{N\hbar^2}{4m}\left(\frac{2}{R_\perp^2} + \frac{1}{R_z^2}\right). \tag{3.10}$$

The kinetic energy is small compared to external potential energy and the interaction energy, when the condensate has sufficiently large number of atoms ($Na/l \gg 1$). This TF regime is the case for most of the BEC experiments, we may therefore safely neglect the kinetic energy term by considering a large cloud.

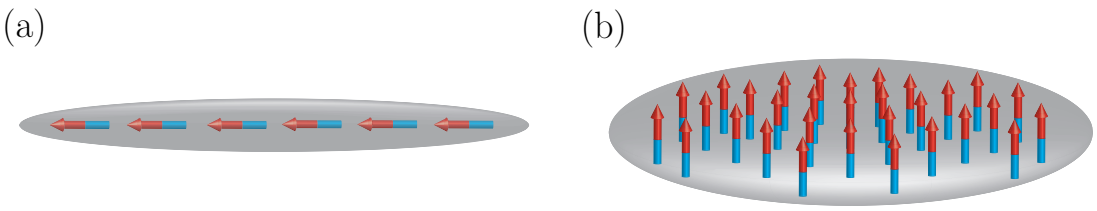

Figure 3.2: Representation of trap geometry and the alignment of dipoles.

3.1.2 Potential Energy Term

External trapping potential is important in determining the geometry of the condensate as dipoles will reconfigure their position depending on the confining potential. For a cigar-shaped trap potential (for which $\omega_x = \omega_y > \omega_z$), the final configuration of dipoles will be the one that they are placed end-to-end along the weak confinement axis (Fig. 3.2a) and the dipolar part of the interparticle interaction will be mostly attractive, whereas for a pancake-shaped trap (for $\omega_x = \omega_y < \omega_z$), the dipoles will be led to locate side by side pointing along the strong confinement axis (Fig. 3.2b), the effect of the dipolar interaction will be mainly repulsive.

Potential Energy corresponds to second term in Eq. (3.5) which is

$$E_{pot} = \int d^3 r V_{tr}(\rho, z)|\psi|^2, \tag{3.11}$$

we substitute for $V_{tr}(\rho, z)$ from Eq. (3.4); for $\psi(\rho, z)$ from Eq. (3.1) to obtain

$$E_{pot} = \pi m \omega_\perp^2 \left(\frac{N}{\pi^{3/2} R_\perp^2 R_z}\right) \underbrace{\int_0^\infty d\rho \rho^3 e^{-\frac{\rho^2}{R_\perp^2}}}_{R_\perp^4/2} \underbrace{\int_{-\infty}^\infty dz e^{-\frac{z^2}{R_z^2}}}_{R_z\sqrt{\pi}}$$

$$+ \pi m \omega_z^2 \left(\frac{N}{\pi^{3/2} R_\perp^2 R_z}\right) \underbrace{\int_0^\infty d\rho \rho e^{-\frac{\rho^2}{R_\perp^2}}}_{R_\perp^2/2} \underbrace{\int_{-\infty}^\infty dz z^2 e^{-\frac{z^2}{R_z^2}}}_{R_z^3\sqrt{\pi}/2}, \tag{3.12}$$

simplifying and arranging terms we get the final expression for the potential energy

$$E_{pot} = \frac{Nm}{2}\left(\omega_\perp^2 R_\perp^2 + \frac{1}{2}\omega_z^2 R_z^2\right). \tag{3.13}$$

3.1.3 Short-Range Interaction Energy Term

Short-range interaction term is due to atom-atom interaction characterized by potential Eq. (2.17) and could be either attractive or repulsive depending on the sign of the scattering length a. Substituting for ψ from Eq. (3.1) into the expression for E_1^{int}, contact interaction term reads

$$\begin{aligned} E_1^{int} &= \int d^3r \frac{g}{2}|\psi|^4 \\ &= \pi g \left(\frac{N}{\pi^{3/2}R_\perp^2 R_z}\right)^2 \underbrace{\int_0^\infty d\rho\rho e^{-2\rho^2/R_\perp^2}}_{R_\perp^2/4} \underbrace{\int_{-\infty}^\infty dz e^{-2z^2/R_z^2}}_{R_z\sqrt{\frac{\pi}{2}}} \\ &= \frac{gN^2}{4\sqrt{2}\pi^{3/2}R_\perp^2 R_z}. \end{aligned} \tag{3.14}$$

Repulsive interactions tend to increase the radius of the condensate and flatten the central density, while the attractive interactions has exactly the opposite trend. Attractive interactions yields in the unstablity of the condensate based on the competition between the strengths of the remaining terms in the energy functional (3.2).

3.1.4 Long-Range Interaction Energy Term

Long range interaction term is the contribution to the energy from the dipoles within the cloud and differs the dipolar gas from the Bose gas with pure contact interactions.

Calculation of the long-range interaction term E_2^{int} is not as straightforward as other terms in Eq. (3.2). We now depict the calculation steps of this term in more detail. The dipolar interaction energy term is

$$E_2^{int} = \frac{1}{2}\int d^3r n(r) \int d^3r' n(r') V_{dd}(r-r') \tag{3.15}$$

where $n(r) = |\psi(r)|^2$ and $n(r') = |\psi(r')|^2$. Substituting densities and dipolar

potential in Eq. (2.52) into Eq. (3.15)

$$E_2^{int} = \frac{C_{dd}}{8\pi}\left(\frac{N}{\pi^{3/2}R_\perp^2 R_z}\right)^2 \int dxdydz e^{\frac{1}{R_\perp^2}(-x^2-y^2)-\frac{z^2}{R_z^2}} \times \int dx'dy'dz' e^{\frac{1}{R_\perp^2}(-x'^2-y'^2)-\frac{z'^2}{R_z^2}} \times \frac{(x'-x)^2+(y'-y)^2-2(z'-z)^2}{\left[(x'-x)^2+(y'-y)^2+(z'-z)^2\right]^{5/2}} \tag{3.16}$$

carrying out the following change of variables

$$\begin{aligned} x'' = x' - x &\implies dx'' = dx' \\ y'' = y' - y &\implies dy'' = dy' \\ z'' = z' - z &\implies dz'' = dz', \end{aligned} \tag{3.17}$$

and inserting into Eq. (3.16)

$$\begin{aligned} E_2^{int} =& \frac{C_{dd}}{8\pi}\left(\frac{N}{\pi^{3/2}R_\perp^2 R_z}\right)^2 \int dxdydz e^{\frac{1}{R_\perp^2}(-x^2-y^2)-\frac{z^2}{R_z^2}} \\ &\times \int dx''dy''dz'' e^{-\frac{(x''+x)^2}{R_\perp^2}-\frac{(y''+y)^2}{R_\perp^2}-\frac{(z''+z)^2}{R_z^2}} \\ &\times \frac{(x'')^2+(y'')^2-2(z'')^2}{\left[(x'')^2+(y'')^2+(z'')^2\right]^{5/2}}, \end{aligned} \tag{3.18}$$

expanding exponential powers in the outer integral and simplifying further

$$\begin{aligned} E_2^{int} = \frac{C_{dd}}{8\pi}\left(\frac{N}{\pi^{3/2}R_\perp^2 R_z}\right)^2 \int dx''dy''dz'' & \frac{(x'')^2+(y'')^2-2(z'')^2}{\left[(x'')^2+(y'')^2+(z'')^2\right]^{5/2}} e^{-\frac{x''^2}{R_\perp^2}-\frac{y''^2}{R_\perp^2}-\frac{z''^2}{R_z^2}} \\ &\times \left(e^{\frac{x''^2}{2R_\perp^2}} \int_{-\infty}^{\infty} dx e^{\frac{-2}{R_\perp^2}\left(x+\frac{x''}{2}\right)^2}\right) \\ &\times \left(e^{\frac{y''^2}{2R_\perp^2}} \int_{-\infty}^{\infty} dy e^{\frac{-2}{R_\perp^2}\left(y+\frac{y''}{2}\right)^2}\right) \\ &\times \left(e^{\frac{z''^2}{2R_z^2}} \int_{-\infty}^{\infty} dz e^{\frac{-2}{R_z^2}\left(z+\frac{z''}{2}\right)^2}\right), \end{aligned} \tag{3.19}$$

next we carry out the Gaussian integrals (which are simply $R_i\sqrt{\pi/2}$) to have

$$\begin{aligned} E_2^{int} =& \frac{C_{dd}}{8\pi}\left(\frac{N}{\pi^{3/2}R_\perp^2 R_z}\right)^2 \left(\frac{\pi}{2}\right)^{3/2} R_\perp^2 R_z \\ &\times \int dx''dy''dz'' \frac{(x'')^2+(y'')^2-2(z'')^2}{\left[(x'')^2+(y'')^2+(z'')^2\right]^{5/2}} e^{-\frac{x''^2}{2R_\perp^2}-\frac{y''^2}{2R_\perp^2}-\frac{z''^2}{2R_z^2}}, \end{aligned} \tag{3.20}$$

changing of variables $u_x = x''/R_\perp$, $u_y = y''/R_\perp$, $u_z = z''/R_\perp$ and letting

$$\alpha = \frac{R_\perp}{R_z},$$

the long range energy becomes

$$\begin{aligned} E_2^{int} =& \frac{C_{dd}}{8\pi} \frac{N^2}{(2\pi)^{3/2} R_\perp^2 R_z} \\ & \times \underbrace{\int du_x du_y du_z \frac{(u_x)^2 + (u_y)^2 - 2(u_z)^2}{\left[(u_x)^2 + (u_y)^2 + (u_z)^2\right]^{5/2}} e^{-\frac{u_x^2}{2} - \frac{u_y^2}{2} - \frac{\alpha^2 u_z^2}{2}}}_{I(\alpha)}. \end{aligned} \tag{3.21}$$

To simplify the calculation of the integral $I(\alpha)$ appeared in Eq. (3.21), we perform inverse Fourier transform of its integrands specified by functions $f_1(\vec{r})$ and $f_2(\vec{r})$,

$$I(\alpha) = \int dxdydz \underbrace{\frac{(x)^2 + (y)^2 - 2(z)^2}{\left[(x)^2 + (y)^2 + (z)^2\right]^{5/2}}}_{f_1(\vec{r})} \underbrace{e^{-\frac{x^2}{2} - \frac{y^2}{2} - \frac{\alpha^2 z^2}{2}}}_{f_2(\vec{r})}$$

where Fourier transform $\mathscr{F}[f(\vec{r})] = \tilde{f}(\vec{k})$ of function $f(\vec{r})$; inverse Fourier transform $\mathscr{F}^{-1}[\tilde{f}(\vec{k})] = f(\vec{r})$ of $\tilde{f}(\vec{k})$ is defined to be:

$$\tilde{f}(\vec{k}) = \int_{-\infty}^{\infty} d^3 r f(\vec{r}) e^{-i\vec{k}.\vec{r}} \Longleftrightarrow f(\vec{r}) = \frac{1}{(2\pi)^3} \int_{-\infty}^{\infty} d^3 r \tilde{f}(\vec{k}) e^{i\vec{k}.\vec{r}}, \tag{3.22}$$

then the integral $I(\alpha)$ can be written as,

$$\begin{aligned} I(\alpha) &= \int d^3 r \int \frac{d^3 k_1}{(2\pi)^3} f_1(\vec{k}_1) e^{i\vec{k}_1.\vec{r}} \int \frac{d^3 k_2}{(2\pi)^3} f_2(\vec{k}_2) e^{i\vec{k}_2.\vec{r}} \\ &= \int \frac{d^3 k_1 d^3 k_2}{(2\pi)^6} \tilde{f}_1(\vec{k}_1) \tilde{f}_2(\vec{k}_2) \underbrace{\int d^3 r e^{i(\vec{k}_1 + \vec{k}_2).\vec{r}}}_{(2\pi)^3 \delta(\vec{k}_1 + \vec{k}_2)}, \end{aligned} \tag{3.23}$$

and letting $k_1 = k$ we have

$$I(\alpha) = \int \frac{d^3 k}{(2\pi)^3} \tilde{f}_1(\vec{k}) \tilde{f}_2(-\vec{k}). \tag{3.24}$$

We have already calculated $\tilde{f}_1(\vec{k})$ in section 2.7 which is the Fourier transform of the dipole-dipole interaction (except or the constant factor of $C_{dd}/4\pi$)

$$\tilde{f}_1(\vec{k}) = 4\pi \left(cos^2\theta - \frac{1}{3} \right) = 4\pi \left(\frac{k_z^2}{k^2} - \frac{1}{3} \right), \tag{3.25}$$

where we set θ to be the angle between $\vec{k}$ and the polarization direction z. It is simple to calculate Fourier transform of $f_2(\vec{r})$, namely

$$\begin{aligned}
\tilde{f}_2(-\vec{k}) &= \int d\vec{r} f_2(\vec{r}) e^{i\vec{k}.\vec{r}} \\
&= \int_{-\infty}^{\infty} dx e^{ik_x x - x^2/2} \int_{-\infty}^{\infty} dy e^{ik_y y - y^2/2} \int_{-\infty}^{\infty} dz e^{ik_z z - \alpha^2 z^2/2} \\
&= \int_{-\infty}^{\infty} dx e^{-\frac{1}{2}k_x^2} e^{-\frac{1}{2}(x-ik_x)^2} \int_{-\infty}^{\infty} dy e^{-\frac{1}{2}k_y^2} e^{-\frac{1}{2}(x-ik_y)^2} \int_{-\infty}^{\infty} \frac{dz'}{\alpha} e^{-\frac{1}{2}k_z^2/\alpha^2} e^{-\frac{1}{2}(z'-ik_z/\alpha)^2} \\
&= \frac{1}{\alpha} e^{-\frac{1}{2}k_x^2 - \frac{1}{2}k_y^2 - \frac{1}{2}k_z^2/\alpha^2} \underbrace{\int_{-\infty}^{\infty} dx' e^{-\frac{1}{2}x'^2}}_{\sqrt{2\pi}} \underbrace{\int_{-\infty}^{\infty} dy' e^{-\frac{1}{2}y'^2}}_{\sqrt{2\pi}} \underbrace{\int_{-\infty}^{\infty} dz'' e^{-\frac{1}{2}z''^2}}_{\sqrt{2\pi}}, \quad (3.26)
\end{aligned}$$

with $x' = x - ik_x$, $y' = y - ik_y$, $z' = \alpha z$ and $z'' = z' - ik_z/\alpha$. So we have here (note that from Eq. (3.26) it follows $\tilde{f}_2(-\vec{k}) = \tilde{f}_2(\vec{k})$)

$$\tilde{f}_2(\vec{k}) = \frac{(2\pi)^{3/2}}{\alpha} e^{-\frac{1}{2}k_x^2 - \frac{1}{2}k_y^2 - \frac{1}{2}k_z^2/\alpha^2}. \quad (3.27)$$

Inserting $\tilde{f}_1(\vec{k})$ and $\tilde{f}_2(\vec{k})$ into Eq. (3.24)

$$\begin{aligned}
I(\alpha) &= \frac{4\pi}{(2\pi)^{3/2}\alpha} \int d^3k \left(\frac{k_z^2}{k^2} - \frac{1}{3}\right) e^{-\frac{1}{2}k_x^2 - \frac{1}{2}k_y^2 - \frac{1}{2}k_z^2/\alpha^2} \\
&= \frac{2\sqrt{2\pi}}{\alpha} \int_0^{\infty} dk k^2 \int_{-1}^{1} d(\cos\theta) \left(cos^2\theta - \frac{1}{3}\right) e^{-\frac{k^2}{2}\sin^2\theta - \frac{k^2}{2\alpha^2}\cos^2\theta} \quad (3.28)
\end{aligned}$$

setting $x = \cos\theta$ and $u = \sqrt{1 - (\alpha^2 - 1/\alpha^2)}k$

$$\begin{aligned}
I(\alpha) &= \frac{2\sqrt{2\pi}}{\alpha} \int_{-1}^{1} dx \left(x^2 - \frac{1}{3}\right) \frac{1}{\left(1 - \frac{\alpha^2-1}{\alpha^2}x^2\right)^{3/2}} \underbrace{\int_0^{\infty} du u^2 e^{-\frac{1}{2}u^2}}_{\sqrt{\pi/2}} \\
&= \frac{2\pi}{\alpha} \int_{-1}^{1} dx \frac{x^2 - \frac{1}{3}}{\left(1 - \frac{\alpha^2-1}{\alpha^2}x^2\right)^{3/2}}, \quad (3.29)
\end{aligned}$$

where the integral is calculated (Appendix A) to be

$$\int_{-1}^{1} dx \frac{x^2 - \frac{1}{3}}{\left(1 - \frac{\alpha^2-1}{\alpha^2}x^2\right)^{3/2}} = -\frac{2}{3}\alpha \left[\frac{1 + 2\alpha^2}{1 - \alpha^2} - \frac{3\alpha^2 \operatorname{arctanh}(\sqrt{1 - \alpha^2})}{(1 - \alpha)^{3/2}}\right], \quad (3.30)$$

therefore, the integral $I(\alpha)$ becomes

$$I(\alpha) = -\frac{4\pi}{3} \left[\frac{1 + 2\alpha^2}{1 - \alpha^2} - \frac{3\alpha^2 \operatorname{arctanh}(\sqrt{1 - \alpha^2})}{(1 - \alpha)^{3/2}}\right]. \quad (3.31)$$

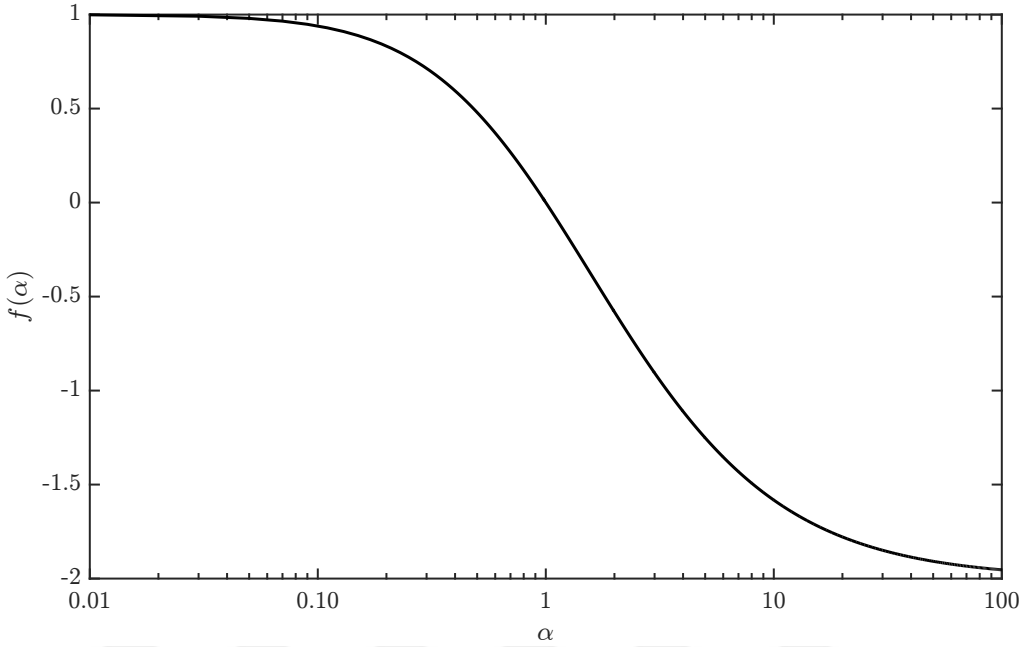

Figure 3.3: The anisotropy function $f(\alpha)$ appearing in the long interaction term.

Substituting Eq. (3.31) into Eq. (3.21), the long-range interaction term reads,

$$E_2^{int} = -\frac{C_{dd}}{6(2\pi)^{3/2}} \frac{N^2}{R_\perp^2 R_z} f(\alpha) \tag{3.32}$$

where,

$$f(\alpha) = \frac{1+2\alpha^2}{1-\alpha^2} - \frac{3\alpha^2 \operatorname{arctanh}(\sqrt{1-\alpha^2})}{(1-\alpha)^{3/2}} \tag{3.33}$$

is the anisotropy function, as the name suggests, it represents the anisotropy property of the dipolar interaction. As can be seen in the Eq. (3.33), this unique feature depends on the trap aspect ratio. A plot of function $f(\alpha)$ is presented in Fig. 3.3, it declines monotically from $f(\alpha = 0) = 1$ to $f(\alpha \to \infty) = -2$ passing zero at $\alpha = 1$. The fact that $f(\alpha)$ vanishes at $\alpha = 1$ implies zero dipolar contribution to the energy when $R_\perp = R_z$. Physically, the dipolar interaction term adds up to zero for spherical density distribution.

3.2 Dimensionless form of the Energy and Parameter Space

In this section we restate the energy in terms of dipolar parameters to address the strengths of the interactions only, to this end we also put the energy into dimensionless form using the following scaling parameters

$$l = \sqrt{\frac{\hbar}{m\bar{\omega}}}, \qquad \bar{\omega} = (\omega_\perp^2 \omega_z)^{1/3},$$

such that

$$\tilde{R}_\perp = \frac{R_\perp}{l}, \qquad \tilde{R}_z = \frac{R_z}{l}, \tag{3.34}$$

where l is the oscillator length which provides order of magnitude for the widths of the condensate; $\bar{\omega}$ is the average trap frequency. Then, the energy equation (3.5) becomes,

$$\tilde{E} = \frac{E}{N\hbar\bar{\omega}} = \frac{1}{4}\left(\frac{2}{\tilde{R}_\perp^2} + \frac{1}{\tilde{R}_z^2}\right) + \frac{1}{4}\left(\frac{\omega_\perp}{\omega_z}\right)^{2/3}\left[2\tilde{R}_\perp^2 + \left(\frac{\omega_z}{\omega_\perp}\right)^2 \tilde{R}_z^2\right]$$

$$+ \frac{1}{2(2\pi)^{3/2}} \frac{gN}{l^3\hbar\bar{\omega}} \frac{1}{\tilde{R}_\perp^2 \tilde{R}_z}\left(1 - \frac{C_{dd}}{3g} f(\alpha)\right). \tag{3.35}$$

Next we define a new set of parameters related to contact and dipolar interactions as well as the anisotropy of the trap, respectively

$$\tilde{g} = \frac{gN}{l^3\hbar\bar{\omega}} = 4\pi\left(\frac{Na}{l}\right), \qquad \epsilon_{dd} = \frac{C_{dd}}{3g}, \qquad \lambda = \frac{\omega_z}{\omega_\perp}. \tag{3.36}$$

The dimensionless parameter ϵ_{dd} is the ratio of the balance between dipolar and contact interactions. It is worth stating that the physics of the dipolar condensate is simply governed by this parameter. The parameter λ is the ratio of the radial frequency $\omega_\perp$ and the frequency along z, ω_z and it is usually called the trap aspect ratio or the trap anisotropy. For a trapped BEC, geometry of

the condensate is determined by the symmetry of the trap. Upon writing the potential (3.4) in terms of λ

$$V_{tr}(\rho, z) = \frac{1}{2} m\omega_{\perp}^2 \left(\rho^2 + \lambda^2 z^2\right), \tag{3.37}$$

we observe that for $\lambda = 1$, the trap is spherical. For $\lambda > 1$, condensate geometry is oblate (pancake-shaped) as $R_{\perp} > R_z$. For $\lambda < 1$, the condensate is prolate (cigar-shaped) as $R_{\perp} < R_z$. In fact, the aspect ratio of the condensate $\alpha = R_{\perp}/R_z$ is same as that of trap λ when the dipolar effects are not switched on ($\epsilon_{dd} = 0$). However when the dipolar interactions are present, the condensate expands depending on the strength of the dipolar interaction and the aspect ratios of trap and the condensate are no longer equal.

We now rewrite the energy equation (3.35) in terms of the dimesionless parameters (3.36)

$$\tilde{E}(\tilde{R}_{\perp}, \tilde{R}_z) = \frac{1}{4}\left(\frac{2}{\tilde{R}_{\perp}^2} + \frac{1}{\tilde{R}_z^2}\right) + \frac{1}{4\lambda^{2/3}}\left[2R_{\perp}^2 + \lambda^2 R_z^2\right]$$

$$+ \frac{1}{2(2\pi)^{3/2}} \frac{\tilde{g}}{\tilde{R}_{\perp}^2 \tilde{R}_z} \left[1 - \epsilon_{dd} f(\alpha)\right], \tag{3.38}$$

in the Thomas-Fermi limit, neglecting the kinetic energy term, which is the first term in Eq. (3.38), the energy as a function of $\alpha = \tilde{R}_{\perp}/\tilde{R}_z$ and $\tilde{R}_z$ reads

$$\tilde{E}(\alpha, \tilde{R}_z) = \frac{\tilde{R}_z^2}{4\lambda^{2/3}}\left[2\alpha^2 + \lambda^2\right] + \frac{1}{2(2\pi)^{3/2}} \frac{\tilde{g}}{\alpha^2 \tilde{R}_z^3} \left[1 - \epsilon_{dd} f(\alpha)\right], \tag{3.39}$$

which is to be minimized to find α.

3.3 Minimization of the Energy with respect to Condensate Radii and the Transcendental Equation

Existence of a global minimum (or local minimum) of the Eq. (3.39) refers to stability (or metastability) of the condensate. To determine the corresponding

stability range, we minimize the Eq. (3.39) with respect to variational parameters α and R_z, respectively, for fixed $\omega_\perp$, ω_z and N

$$\frac{\partial \tilde{E}}{\partial \tilde{R}_z} = \frac{\tilde{R}_z}{2\lambda^{2/3}}\left(2\alpha^2+\lambda^2\right) + \frac{-3}{2(2\pi)^{3/2}}\frac{\tilde{g}}{\alpha^2\tilde{R}_z^4}\left[1-\epsilon_{dd}f(\alpha)\right] = 0, \tag{3.40}$$

Solving for $\tilde{R}_z$ gives

$$\tilde{R}_z = \left\{\frac{3}{(2\pi)^{3/2}}\frac{\tilde{g}\lambda^{2/3}}{\alpha^2(2\alpha^2+\lambda^2)}\left[1-\epsilon_{dd}f(\alpha)\right]\right\}^{1/5}. \tag{3.41}$$

Let us show the radial width as well

$$\tilde{R}_x = \tilde{R}_y = \left\{\frac{3}{(2\pi)^{3/2}}\frac{\alpha^3\tilde{g}\lambda^{2/3}}{(2\alpha^2+\lambda^2)}\left[1-\epsilon_{dd}f(\alpha)\right]\right\}^{1/5}. \tag{3.42}$$

Substituting $\tilde{R}_z$ back into Eq. (3.39), we have

$$\tilde{E}(\alpha) = \frac{5}{3^{3/5}4}\frac{\tilde{g}^{2/5}}{\lambda^{2/5}(2\pi)^{3/5}}\frac{(2\alpha^2+\lambda^2)^{3/5}}{\alpha^{4/5}}\left[1-\epsilon_{dd}f(\alpha)\right]^{2/5}. \tag{3.43}$$

Then (see appendix B for details)

$$\begin{aligned}\frac{\partial \tilde{E}(\alpha)}{\partial \alpha} =& -(2\alpha^2+\lambda^2)\epsilon_{dd}\left[-\frac{2}{\alpha}+\left(\frac{2}{\alpha}+\frac{3\alpha}{1-\alpha^2}\right)f(\alpha)\right] \\ &+\frac{2(\alpha^2-\lambda^2)}{\alpha}\left[1-\epsilon_{dd}f(\alpha)\right] = 0,\end{aligned} \tag{3.44}$$

Further simplification of Eq. (3.44) yields a transcendental equation

$$3\alpha\epsilon_{dd}\left[\left(1+\frac{\lambda^2}{2}\right)\frac{f(\alpha)}{1-\alpha^2}-1\right]+(\alpha^2-\lambda^2)(\epsilon_{dd}-1) = 0, \tag{3.45}$$

which is to be solved graphically determining the condensate aspect ratio α. We note from the transcendental equation (3.45) that, when the dipolar coupling constant ϵ_{dd} is zero, trap aspect ratio and the condensate aspect ratio are the same (i.e. $\lambda = \alpha$, when $\epsilon_{dd} = 0$), this is already what we expect in the absence of dipolar interaction. Eq. (3.45) can be considered as the relation between condensate and trap aspect ratios, we will carry out its graphical solution in section 3.4.

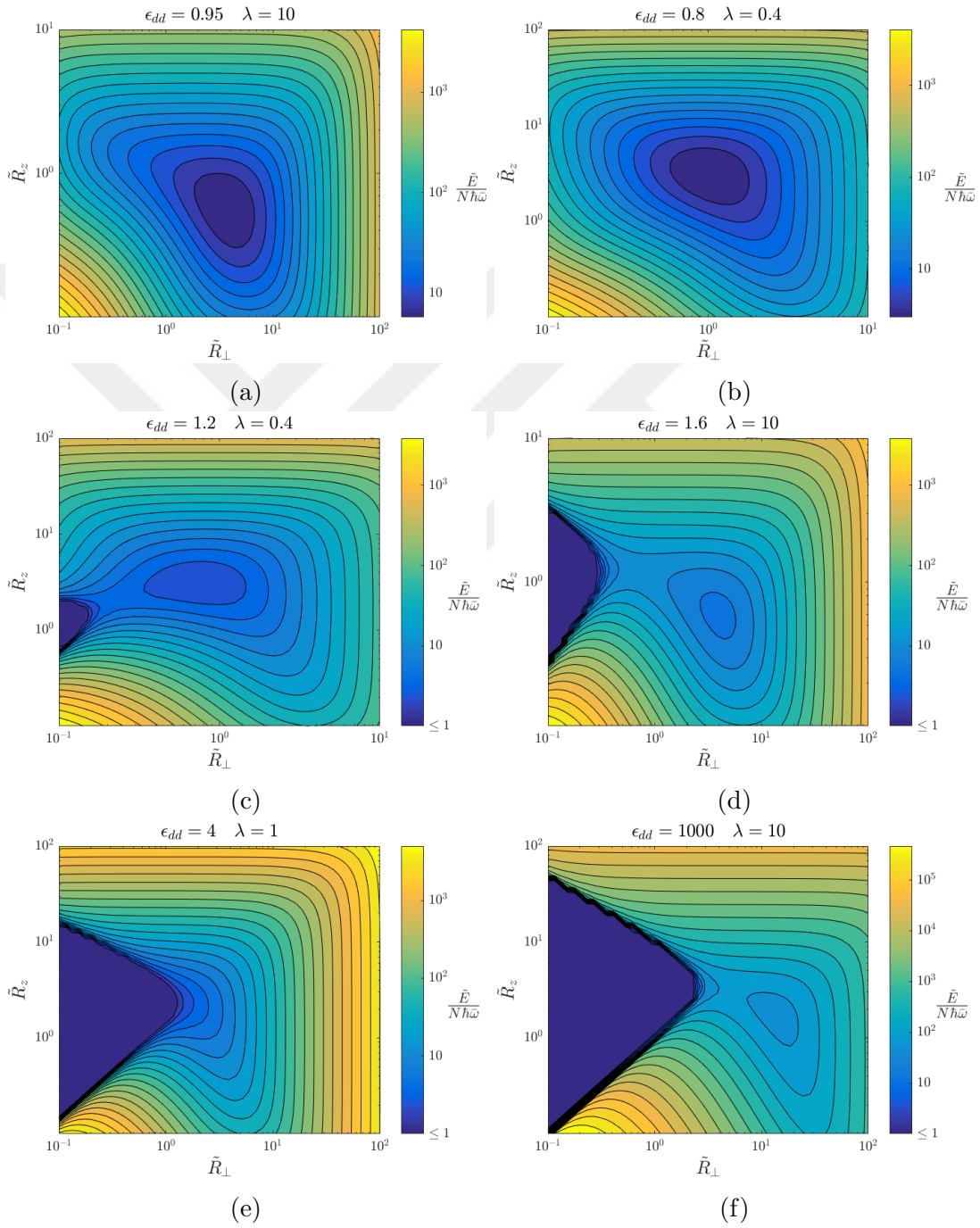

Figure 3.4: Contour plots (energy lanscape) of the dimensionless energy $\tilde{E}(\tilde{R}_\perp, \tilde{R}_z)$ given in Eq. (3.38) for fixed values of $\tilde{g} = 180$; for different values of the parameters ϵ_{dd} and λ as depicted on the figures.

3.4 The stability of the Condensate and the Energy Landscape

To investigate the stability of a condensate, we need to consider the total interaction between the atoms. In the present case, it is the sum of the contact and the dipolar interactions. The total interaction energy of the system is therefore, from the second term of the Eq.(3.39)

$$\tilde{E}_{int} = \tilde{E}_1^{int} + \tilde{E}_2^{int} = \frac{1}{2(2\pi)^{3/2}} \frac{\tilde{g}}{\alpha^2 \tilde{R}_z^3} \left[1 - \epsilon_{dd} f(\alpha)\right], \tag{3.46}$$

there are two possibilities for the total interparticle interaction: it could be either repulsive or attractive. In the case of attractive interactions the central density of the gas tends to increase in order to reduce the interaction energy, however if the central density increases more than the kinetic energy can balance, as a result the gas start to collapse; for repulsive interactions, on the other hand, the collapse is not the case, therefore yielding a stable gas. Accordingly, for the gas to be stable we expect repulsive total interaction which implies $\tilde{E}_{int} > 0$, leading to the condition

$$[1 - \epsilon_{dd} f(\alpha)] > 0 \implies \epsilon_{dd} < 1/f(\alpha). \tag{3.47}$$

For an highly cigar-shaped condensate, condensate aspect ratio approaches to zero ($\alpha = R_\perp/R_z \to 0$), but the anisotropy function in this limit reads $f(\alpha \to 0) = 1$, therefore the ratio of the dipolar and s-wave coupling strengths should satisfy, from the Eq. (3.47), $\epsilon_{dd} < 1$. Additionally, to observe dipolar effects one should not neglect ϵ_{dd}, when this parameter vanishes, we have a non-dipolar gas with pure s-wave interactions. Consequently, we may expect the stability interval to be $0 \leq \epsilon_{dd} < 1$.

In fact, transcendental equation (3.45) has a unique solution α for any chosen value of the trap aspect ratio λ in the interval $0 \leq \epsilon_{dd} < 1$ (Fig. 3.5), consistent with our presumed stability range for ϵ_{dd}. The solutions given in this range corresponds to global minimum in the energy landscape (Fig. 3.4a, Fig. 3.4b), meaning that in this range the condensate is stable. As we start increasing ϵ_{dd} from unity, the transcendental equation (3.45) gives multiple solutions for α

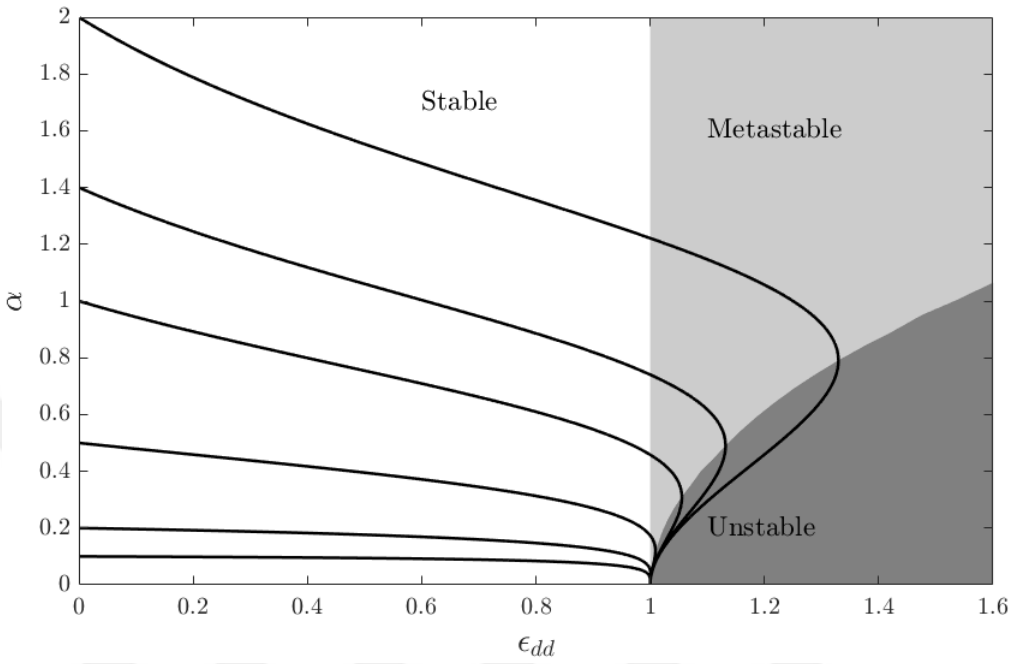

(a)

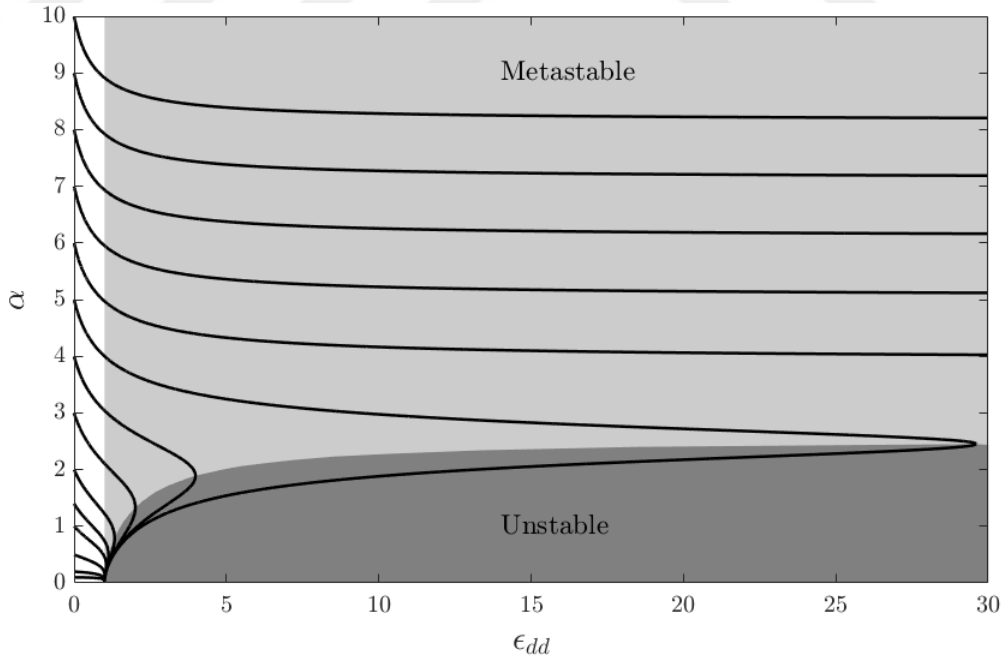

(b)

Figure 3.5: Figures represent the graphical solution of the transcendental equation (3.45) with each line representing different values of the trap aspect ratio λ; values of α are represented as a function of ϵ_{dd}. The condensate is always stable in the interval $0 \leq \epsilon_{dd} < 1$, for bigger values of ϵ_{dd} condensate is either metastable or unstable as depicted on the graphs. Figures are derived from [58] (where obtained for Thomas-Fermi density) for a Gaussian density profile.

(Fig. 3.5), the one branch of solutions is seen as only having a local minimum in the energy landscape (Fig. 3.4c, Fig. 3.4d) and the global minimum is a metastable collapsed state as $\alpha \to 0$; the other branch of solutions corresponds to saddle points in the energy landscape, at the sufficiently larger values of ϵ_{dd} (can be seen in Fig. 3.5b), there is a critical value for trap aspect ratio λ below which solutions are either metastable or unstable up to a critical value for ϵ_{dd}, increasing ϵ_{dd} further above the critical value even the local minimum vanishes (Fig. 3.4e) meaning that there are no solutions to the transcendental equation (3.45), this corresponds to a collapsed state with $\alpha = 0$. However, if the trap aspect ratio λ is higher than the critical value, solutions correspond to metastable ones as is shown for several values (e.g. for $\lambda = 6, 7, 8, 9, 10$) in Fig. 3.5b and in the energy landscape Fig. 3.4f.

From the Fig. 3.5, information regarding the relation between geometry of the trap and the stability of the condensate can also be extracted considering the fact that for $0 < \lambda < 1$ ($0 < \alpha < 1$) the trap (condensate) is prolate; when $\lambda > 1$ ($\alpha > 1$) the trap (condensate) is oblate. In this section we have examined the geometry dependence of stability including both cases of prolate trap and oblate trap, and our discussion based on the transcendental equation (3.45) and the Fig. 3.5 that represents its solution which enabled us to interpret a wide range of the results regardless of the specific geometry. In particular, we desire to conclude this section by underlining the case of cigar-shaped (prolate) trap which corresponds to data plotted in Fig. 3.5a for the values $\alpha\ (= \lambda(\epsilon_{dd} = 0)) < 1$. We observe that within the range $0 \leq \epsilon_{dd} < 1$, the condensate is always stable which implies a global minimum in the energy landscape, whereas for values increased from 1, the condensate is either metastable or unstable that corresponds to a local minimum along with the saddle points, in the energy landscape.

3.5 Connection to the Thomas-Fermi Solution

Study of Thomas-Fermi approximated BEC with dipolar interactions, requires mathematically more demanding manipulations compared to the BEC with only

contact interactions. However, the former case has been analyzed in reference [58] and a remarkable result emerged: dipole-dipole mean-field potential has only quadratic or constant terms, meaning that the density profile is inverted-parabola like, just as in the case of pure contact interactions.

In the Thomas-Fermi calculation of the dipolar gas the following ansatz is used for density profile

$$n(\vec{r}) = \frac{15N}{8\pi R_\perp^2 R_z}\left(1 - \frac{\rho^2}{R_\perp^2} - \frac{z^2}{R_z^2}\right), \tag{3.48}$$

where condensate radii are $R_x = R_y$ and R_z. The equilibrium widths of the condensate is given by

$$R_x = \left\{\frac{15gN\alpha}{4\pi m\omega_\perp^2}\left[1 + \epsilon_{dd}\left(\frac{3}{2}\frac{\alpha^2 f(\alpha)}{1-\alpha^2} - 1\right)\right]\right\}^{1/5}, \tag{3.49}$$

where $R_z = R_x/\alpha$. The condensate aspect ratio α is also determined by the same transcendental equation (3.35) that we derived for a Gaussian density profile. Therefore, we find that the aspect ratio is insensitive to the type of the density profile.

It is useful to demonstrate the following delta-function identity analogous to the Laplacian of $1/r$, namely $\nabla^2(1/r) = -4\pi\delta(\vec{r})$

$$\partial_i\partial_j\frac{1}{r} = \frac{3\hat{r}_i\hat{r}_j - \delta_{ij}}{r^3} - \frac{4\pi}{3}\delta_{ij}\delta(\vec{r}). \tag{3.50}$$

Identity (3.50) was first derived in reference [62] and it enables us to rewrite the dipole-dipole potential (2.43) in a more handy way. Substituting the Eq.(3.50) into Eq.(2.43) we get

$$\begin{aligned} V_{dd}(\vec{r}) &= \frac{C_{dd}}{4\pi}\hat{e}_i\hat{e}_j\frac{(\delta_{ij} - 3\hat{r}_i\hat{r}_j\delta(\vec{r}))}{r^3} \\ &= -C_{dd}\hat{e}_i\hat{e}_j\left(\partial_i\partial_j\frac{1}{4\pi r} + \frac{\delta_{ij}\delta(\vec{r})}{3}\right). \end{aligned} \tag{3.51}$$

Next, we substitute Eq. (3.51) into the expression for the dipole-dipole mean-field

potential (3.3)

$$\begin{aligned}\Phi_{dd} &= \int d^3r' V_{dd}(\vec{r}-\vec{r'})n(\vec{r'}) \\ &= -C_{dd}\hat{e}_i\hat{e}_j\Big(\partial_i\partial_j\frac{1}{4\pi}\underbrace{\int d^3r'\frac{n(\vec{r'})}{|\vec{r}-\vec{r'}|}}_{\phi(\vec{r})} + \frac{\delta_{ij}}{3}\underbrace{\int d^3r'\delta(\vec{r}-\vec{r'})n(\vec{r'})}_{n(\vec{r})}\Big) \\ &= -C_{dd}\hat{e}_i\hat{e}_j\left(\partial_i\partial_j\phi(\vec{r}) + \frac{\delta_{ij}}{3}n(\vec{r})\right). \end{aligned} \tag{3.52}$$

We observe from Eq. (3.52) that mean field dipolar potential can be calculated in a similar way that we calculate the electric potential due to a volume charge, provided that the function $\phi(\vec{r})$ satisfies the Poisson's equation, i.e. $\nabla^2\phi(\vec{r}) = -n(\vec{r})$. In general, Eq. (3.52) ensures the simplification of the original integral (3.3) to be solved analytically and simplifies the visualization of the problem by reducing it to the electrostatic counterpart.

3.6 Elongation of the Condensate

We have intuitively assumed that the condensate will elongate in the direction of dipoles along which we set the trapping potential less strongly compared to the radial direction. The attractive ($\alpha < 1$) and the repulsive ($\alpha > 1$) nature of the dipolar interaction term has led us to this guess. In fact, it is reasonable once we remember the fact that dipoles in a head to tail configuration will tend to attract one another while adjoining dipoles repel each other. Considering the instant before we switch on the trap potential, randomly located dipoles within the cloud will tend to reconfigure their position in such a way that the energy of this system will be minimum. This configuration can be visualized by a straightforward example where we examine the dipolar potential in the case of an isotropic cloud. In this example, we use the following isotropic TF density

$$n(r) = \frac{m\omega_0 R^2}{2g}\left(1 - \frac{r^2}{R^2}\right), \tag{3.53}$$

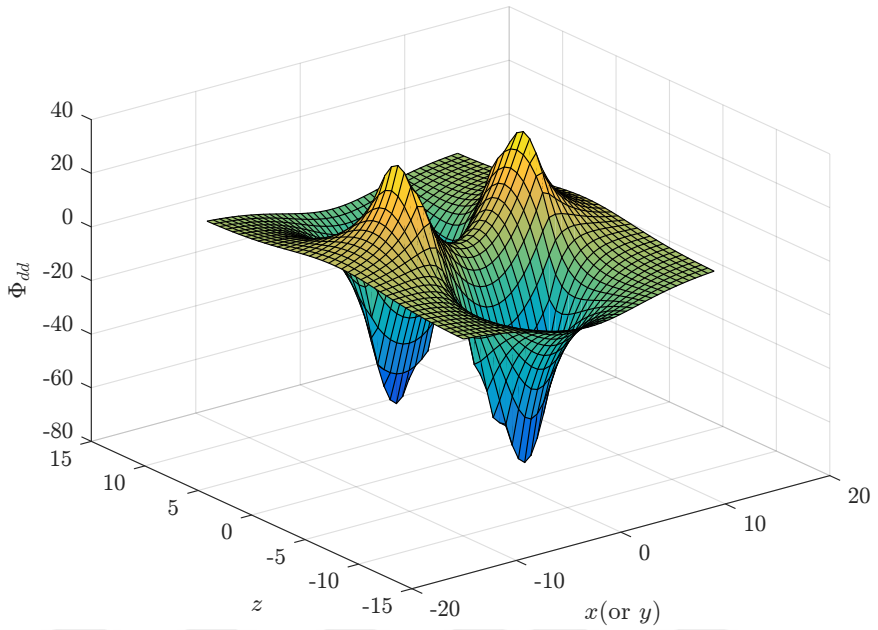

Figure 3.6: Plot of the dipolar potential Φ_{dd} for constant y (or x) in the case of a sperically symmetric trap.

and polarize the dipoles along z direction. The ϕ function for density (3.53) is calculated in spherical coordinates to be (appendix B)

$$\phi(r) = \frac{m\omega_0^2 R^2}{4gr} \int_0^R dr' r' \left(1 - \frac{r'^2}{R^2}\right) \left[r + r' - |r - r'|\right]. \tag{3.54}$$

In the outside region ($r > R$), the integral (3.54), as $|r - r'| = r - r'$, reads

$$\phi_{out}(r) = \frac{m\omega_0^2 R^2}{2gr} \int_0^R dr' r'^2 \left(1 - \frac{r'^2}{R^2}\right) = \frac{m\omega_0^2}{15g} \frac{R^5}{r}. \tag{3.55}$$

For the inside region ($r < R$), we have to split the integration into two parts for $0 \leq r' < r$ and $r < r' \leq R$, namely

$$\phi_{in}(r) = \frac{m\omega_0^2 R^2}{2gr} \left[\int_0^r dr' r'^2 \left(1 - \frac{r'^2}{R^2}\right) + \int_r^R dr' r' r \left(1 - \frac{r'^2}{R^2}\right)\right]$$

$$= \frac{m\omega_0^2 R^2}{2g} \left(-\frac{R^2 r^2}{6} + \frac{r^4}{20} + \frac{R^4}{2}\right). \tag{3.56}$$

Having calculated the ϕ functions appearing in Eq. (3.52), we next find the corresponding dipolar mean-field potential in all space. We begin with substituting Eq. (3.55) into Eq. (3.52) with second term ($\sim n(r)/3$) being zero as density

$n(r)$ is clearly zero outside the condensate. The dipolar potential for $r > R$ then reads

$$\begin{aligned}\Phi_{dd}^{out}(r) &= -C_{dd}\hat{z}\cdot\hat{z}\left(\partial_z\partial_z\phi(\vec{r}) + \frac{\delta_{ij}}{3}\underbrace{n(\vec{r})}_{=0}\right)\\ &= -\frac{m\omega_0^2R^5}{15g}C_{dd}\left(\partial_z^2\frac{1}{r}\right)\\ &= -\frac{m\omega_0^2R^5}{15g}C_{dd}\left(-\frac{1-3z^2/r^2}{r^3}\right)\\ &= \epsilon_{dd}\frac{m\omega_0^2}{5}(1-3\cos^2\theta)\frac{R^5}{r^3}.\end{aligned} \tag{3.57}$$

For the interior ($r < R$) of the condensate, we insert the Eq. (3.56) into Eq. (3.52) to find the potential inside

$$\begin{aligned}\Phi_{dd}^{in}(r) &= -\frac{m\omega_0^2}{2g}C_{dd}\left[\partial_z^2\left(-\frac{R^2r^2}{6}+\frac{r^4}{20}\right)+\frac{1}{3}\left(R^2-r^2\right)\right]\\ &= \frac{m\omega_0^2}{15g}C_{dd}\left[\left(1-3\frac{z^2}{r^2}\right)r^2\right]\\ &= \epsilon_{dd}\frac{m\omega_0^2}{5}(1-3\cos^2\theta)r^2.\end{aligned} \tag{3.58}$$

Consequently, we have calculated the dipolar mean-field potential over all space resulting in

$$\Phi_{dd}(r) = \epsilon_{dd}\frac{m\omega_0^2}{5}(1-3\cos^2\theta)\begin{cases} r^2, & \text{if } r < R,\\ \frac{R^5}{r^3}, & \text{if } r > R.\end{cases} \tag{3.59}$$

Plot of Φ_{dd} (Fig. 3.6) shows that it has a minimum on the z-axis along which we polarized the dipoles, therefore energetically most favorable configuration for the condensate is to elongate along z (orientation direction of dipoles). Elongation will increase with increasing ϵ_{dd}. This qualitative evaluation remains valid for anisotropic case which has been examined in reference [58].

Chapter 4

Generalization of the Problem: Separate Directions for Dipole Orientation and Trap Symmetry

In this chapter we wish to further investigate the effect of the geometry on the stability of the condensate. For this purpose, we designate separate directions for the dipole orientation and the symmetry axis of the trap by applying the external field along a new direction specified by an angle γ from the positive z direction, which is a result of rotation around y, as depicted in Fig. 4.1. In the present case, we will be dealing with three cartesian coordinates r, r', r'' where the last two are obtained by consecutive rotations around y axis by an angle of β and γ, respectively (Fig. 4.1). Among these coordinates, primed ones correspond to the elongation direction of the condensate, double primed coordinates are where the dipoles lie and the unprimed ones peculiar to the external trapping potential. The configuration discussed above and represented in (Fig. 4.1) follows from the fact that the trap, which has a weak confinement direction along z axis will tend to elongate the condensate along its own symmetry whereas the dipoles oriented along z'' direction will cause an elongation along z''. Therefore, we expect the overall effect stemming from these two interactions to be a total elongation in-between, which corresponds to the direction z' characterized by the angle β

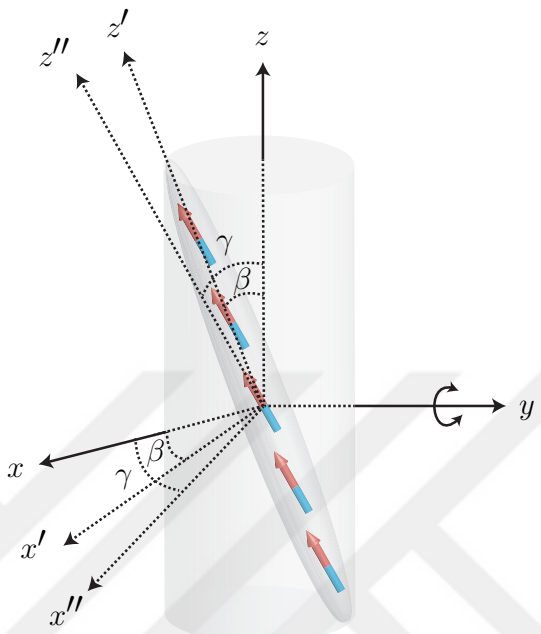

Figure 4.1: The schematic representation of the new problem, where we assign separate directions for the alignment of dipoles and the weak confinement direction of the cylindrically symmetric trap.

that will serve as the new variational parameter for the present problem. It is instructive to stress that, as far as the problem is concerned, γ is an arbitrary angle along which we point the external polarizing field, however we expect there to be a certain relation between γ and β.

There are several issues that we should pay attention to, first one is that we have three coordinates (all having the same y axis) but obviously we have to work only in one of them. To do that, we can rotate any coordinates to the other one so that condensate wave function and the dipolar interaction and the trap potential all lie in the same space. Nevertheless, not all of the choices result in analytically (or numerically easily) solvable integrals. The most preferable way for the simplicity of the calculations is that we rotate primed coordinates to the double primed coordinates, in other words, we rotate the coordinate space that the condensate wave function rests, along the alignment direction of the dipoles. In addition, for kinetic and potential energies, final state of the condensate matters which corresponds to an elongated condensate along z' and specified by the

angle β from the trap symmetry axis z.

We have organized this chapter as follows: As the first step we calculate the energy of the system in the condensate space (primed coordinates) based on a variational approach by carrying out the necessary rotations. However, calculation of the long range interactions (due to an hard-to-solve integral) is even more tedious compared to the case presented in chapter 3, we will demonstrate each step and the techniques used explicitly. We will then investigate the effect of this new geometry on the stability of the condensate.

4.1 Obtaining the Energy Equation

For the present problem, we will be utilizing the following Gaussian ansatz which is normalized to N

$$\psi(x',y',z') = \sqrt{\frac{N}{\pi^{3/2}R_xR_yR_z}}e^{-x'^2/2R_x^2-y'^2/2R_y^2-z'^2/2R_z^2}, \tag{4.1}$$

where primed coordinates correspond to the new elongation direction of the condensate (compared to the discussion made in chapter 3) which can be stated polarization direction of dipoles as following

$$\begin{aligned} x' &= x''\cos(\gamma-\beta)+z''\sin(\gamma-\beta) \\ y' &= y'' \\ z' &= z''\cos(\gamma-\beta)-x''\sin(\gamma-\beta), \end{aligned} \tag{4.2}$$

and the Gaussian integrals related to this trial wave function

$$\begin{aligned} \int_{-\infty}^{\infty} dj' j'^2 e^{-j'^2/R_j^2} &= R_j^3\sqrt{\frac{\pi}{2}}, \\ \int_{-\infty}^{\infty} dj' j' e^{-j'^2/R_j^2} &= 0, \\ \int_{-\infty}^{\infty} dj' e^{-j'^2/R_j^2} &= R_j\sqrt{\pi}, \end{aligned} \tag{4.3}$$

where $j = x, y, z$. As referred to previously, we again employ the harmonic oscillator length l, average trap frequency $\bar{\omega} = (\omega_\perp^2 \omega_z)^{1/3}$ and average oscillator energy $N\hbar\bar{\omega}$ of the gas to put the equations in dimensionless form.

We now variationally calculate the energy by utilizing the functional (3.2) term by term explicitly presenting the calculation steps.

4.1.1 Kinetic Energy

In obtaining the kinetic energy, we should be cautious about the coordinates we use and consider the fact that it is the kinetic energy of the condensate of which final configuration will be a cigar-shape form oriented along z'. The kinetic energy term then reads

$$E_{kin} = \int d^3r' |\vec{\nabla}\psi(x', y', z')|^2, \tag{4.4}$$

with

$$\begin{aligned} |\vec{\nabla}\psi|^2 &= \left| \hat{x}\frac{\partial}{\partial x'}\psi + \hat{y}\frac{\partial}{\partial y'}\psi + \hat{z}\frac{\partial}{\partial z'}\psi \right|^2 \\ &= \left(\hat{x}\frac{\partial}{\partial x'}\psi + \hat{y}\frac{\partial}{\partial y'}\psi + \hat{z}\frac{\partial}{\partial z'}\psi \right)^* \cdot \left(\hat{x}\frac{\partial}{\partial x'}\psi + \hat{y}\frac{\partial}{\partial y'}\psi + \hat{z}\frac{\partial}{\partial z'}\psi \right) \\ &= \left| \frac{\partial\psi}{\partial x'} \right|^2 + \left| \frac{\partial\psi}{\partial y'} \right|^2 + \left| \frac{\partial\psi}{\partial z'} \right|^2, \end{aligned} \tag{4.5}$$

where the derivatives of ψ appearing in Eq. (4.5), for $j = x, y, z$, are

$$\frac{\partial\psi}{\partial j'} = -\frac{j'}{R_j^2}\psi, \tag{4.6}$$

then

$$|\vec{\nabla}\psi|^2 = \frac{x'^2}{R_x^4}|\psi|^2 + \frac{y'^2}{R_y^4}|\psi|^2 + \frac{z'^2}{R_z^4}|\psi|^2, \tag{4.7}$$

inserting equation Eq. (4.7) into Eq. (4.4) we get

$$
\begin{aligned}
E_{kin} = \frac{\hbar^2}{2m}\frac{N}{\pi^{3/2}R_xR_yR_z} \\
\times\Bigg[\frac{1}{R_x^4}\left(\int_{-\infty}^{\infty}dx'x'^2e^{-x'^2/R_x^2}\right)\left(\int_{-\infty}^{\infty}dy'e^{-y'^2/R_y^2}\right)\left(\int_{-\infty}^{\infty}dz'e^{-z'^2/R_z^2}\right) \\
+\frac{1}{R_x^4}\left(\int_{-\infty}^{\infty}dx'e^{-x'^2/R_x^2}\right)\left(\int_{-\infty}^{\infty}dy'y'^2e^{-y'^2/R_y^2}\right)\left(\int_{-\infty}^{\infty}dz'e^{-z'^2/R_z^2}\right) \\
+\frac{1}{R_x^4}\left(\int_{-\infty}^{\infty}dx'e^{-x'^2/R_x^2}\right)\left(\int_{-\infty}^{\infty}dy'e^{-y'^2/R_y^2}\right)\left(\int_{-\infty}^{\infty}dz'z'^2e^{-z'^2/R_z^2}\right)\Bigg],
\end{aligned}
$$

substituting corresponding values of the Gaussian integrals in round brackets from Eq. (4.3) and simplifying we have

$$E_{kin} = \frac{N\hbar^2}{4m}\left(\frac{1}{R_x^2}+\frac{1}{R_y^2}+\frac{1}{R_z^2}\right). \tag{4.8}$$

For a qualitative analysis, we will later assume equal radial radii such that $R_x = R_y = R_\perp$, in that case kinetic energy reads, as in the previous case,

$$E_{kin} = \frac{N\hbar^2}{4m}\left(\frac{2}{R_\perp^2}+\frac{1}{R_z^2}\right). \tag{4.9}$$

4.1.2 Potential Energy

The potential energy term due to trap potential is calculated in the similar manner as we did in calculating the kinetic energy, the difference is that due to the unprimed coordinates dependent external potential, the potential energy will be a function of the variational parameter β, as well (along with the parameters $R_\perp$ and R_z), namely

$$E_{pot} = \int d^3r' V_{tr}(x,y,z)|\psi(x',y',z')|^2, \tag{4.10}$$

we calculate the energy in primed coordinates along which we expect condensate to elongate, while the trap potential

$$V_{tr}(x,y,z) = \frac{1}{2}m\omega_\perp^2(x^2+y^2)+\frac{1}{2}m\omega_z^2z^2 \tag{4.11}$$

is in unprimed coordinates. We employ a rotation to write the potential in accordance with the primed condensate coordinates. From the Fig.4.1 we can write

$$\begin{aligned} x &= z' \sin\beta + x' \cos\beta \\ y &= y' \\ z &= z' \cos\beta - x' \sin\beta, \end{aligned} \tag{4.12}$$

therefore, the external potential becomes

$$\begin{aligned} V_{tr}(x,y,z) &= \frac{1}{2} m\omega_\perp^2 \left[(z' \sin\beta + x' \cos\beta)^2 + y'^2 \right] \\ &\quad + \frac{1}{2} m\omega_z^2 \left(z' \cos\beta - x' \sin\beta \right)^2 \\ &= \frac{1}{2} m(\omega_\perp^2 \cos^2\beta + \omega_z^2 \sin^2\beta) x'^2 + \frac{1}{2} m\omega_\perp^2 y'^2 \\ &\quad + \frac{1}{2} m(\omega_\perp^2 \sin^2\beta + \omega_z^2 \cos^2\beta) z'^2 + m(\omega_\perp^2 - \omega_z^2) x' z' \cos\beta \sin\beta \end{aligned} \tag{4.13}$$

next, we insert this trap potential into the expression for the potential energy term (4.10)

$$\begin{aligned} E_{pot} =& \frac{N}{\pi^{3/2} R_x R_y R_z} \left[\frac{1}{2} m\omega_\perp^2 \left(\int_{-\infty}^{\infty} dx' x'^2 e^{-x'^2/R_x^2} \right) \right. \\ &\times \left(\int_{-\infty}^{\infty} dy' e^{-y'^2/R_y^2} \right) \left(\int_{-\infty}^{\infty} dz' e^{-z'^2/R_z^2} \right) \\ &+ \frac{1}{2} m(\omega_\perp^2 \cos^2\beta + \omega_z^2 \sin^2\beta) \left(\int_{-\infty}^{\infty} dx' x'^2 e^{-x'^2/R_x^2} \right) \\ &\times \left(\int_{-\infty}^{\infty} dy' e^{-y'^2/R_y^2} \right) \left(\int_{-\infty}^{\infty} dz' e^{-z'^2/R_z^2} \right) \\ &+ \frac{1}{2} m(\omega_\perp^2 \sin^2\beta + \omega_z^2 \cos^2\beta) \left(\int_{-\infty}^{\infty} dx' x'^2 e^{-x'^2/R_x^2} \right) \\ &\times \left. \left(\int_{-\infty}^{\infty} dy' e^{-y'^2/R_y^2} \right) \left(\int_{-\infty}^{\infty} dz' e^{-z'^2/R_z^2} \right) \right], \end{aligned} \tag{4.14}$$

substituting for the Gaussian integrals in round brackets from Eq. (4.3) and simplifying, we get the following expression for the potential energy

$$E_{pot} = \frac{Nm}{4} \left[\omega_\perp^2 R_y^2 + (\omega_\perp^2 \cos^2\beta + \omega_z^2 \sin^2\beta) R_x^2 + (\omega_\perp^2 \sin^2\beta + \omega_z^2 \cos^2\beta) R_z^2 \right], \tag{4.15}$$

One can readily notice that, if we take the parameter β to be zero by aligning the external field along the trap symmetry axis z, potential energy (4.15) is identical to one in the previous problem of chapter 3 when $R_x = R_y$.

4.1.3 Contact Energy and Long-Range Interaction Energy for the case $R_x = R_y$

In particular, long-range energy interaction and the external potential terms of the energy functional is affected from the new geometry we have defined in this chapter, while the kinetic and contact interaction terms are identical to the previous case (when $R_x = R_y = R_\perp$) in chapter 2. In the new symmetry, we expect the radial widths R_x and R_y to be different from each other as the elongations along dipole direction and trap anisotropy directions will not be at the same rate. However, investigating the case as if the radial radii are equal will serve as a fruitful qualitative analysis and suffice for our purposes. The problem is schematically pictured in Fig. 4.1 and the dipolar interaction term due to pair of dipoles which lies in the double-primed coordinate space can be be visualized as in (Fig. 4.2), and this interaction is characterized, as usual, by the following expression

$$V_{dd} = \frac{C_{dd}}{4\pi} \frac{(x_2 - x_1)^2 + (y_2 - y_1)^2 - 2(z_2 - z_1)^2}{[(x_2 - x_1)^2 + (y_2 - y_1)^2 + (z_2 - z_1)^2]^{5/2}}. \tag{4.16}$$

Firstly, we calculate the contact energy of the condensate due to binary interactions of the constituent particles,

$$\begin{aligned} E_1^{int} =& \frac{g}{2} \int d^3r' |\psi(x', y', z')|^4 \\ =& \frac{1}{2} \left(\frac{N}{\pi^{3/2} R_x R_y R_z} \right)^2 \int_{-\infty}^{\infty} dx' e^{-2x'^2/R_x^2} \\ & \times \int_{-\infty}^{\infty} dy' e^{-2y'^2/R_y^2} \int_{-\infty}^{\infty} dz' e^{-2z'^2/R_z^2}, \end{aligned} \tag{4.17}$$

substituting for the Gaussion integrals from equation (4.3), contact energy reads

$$E_1^{int} = \frac{N^2}{2(2\pi)^{3/2}} \frac{g}{R_x R_y R_z}. \tag{4.18}$$

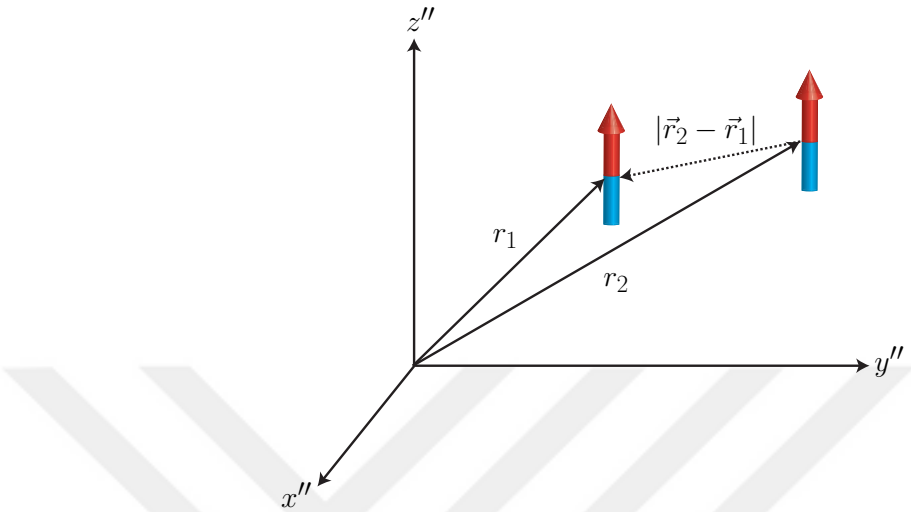

Figure 4.2: Cartesian coordinate space where the dipoles within the condensate lie.

As a next step, we systematically calculate the long-range interaction energy with $R_x = R_y = R_\perp$. Manipulations made in the rest of this section is formulized in terms of some new dimensionless parameters (α, A, B, C, D, a, b, d, S, K, κ, ν, μ, ϵ, η) and every single one of them has the purpose of introducing harmony to equations and ease to the numerical calculations of which results will be shown at the end of the present chapter. The density ansatz that we use for the calculation of the long-range energy follows from the Eq. (4.1) and Eq. (4.2) to be

$$n(r'') = \frac{N}{\pi^{3/2} R_\perp^2 R_z} e^{-Ax''^2/R_\perp^2 - y''^2/R_\perp^2 - Bz''^2/R_\perp^2 - 2Cx''z''/R_\perp^2} \tag{4.19}$$

where

$$\begin{aligned} \alpha &= R_\perp/R_z, \\ A &= \cos^2(\gamma-\beta) + \alpha^2 \sin^2(\gamma-\beta), \\ B &= \sin^2(\gamma-\beta) + \alpha^2 \cos^2(\gamma-\beta), \\ C &= (1-\alpha^2)\sin(\gamma-\beta)\cos(\gamma-\beta). \end{aligned} \tag{4.20}$$

Then, for the long-range interaction energy with the interaction (4.16) and density (4.19) we have

$$E_2^{int} = \frac{1}{2}\int d^3r_1 n(r_1)\int d^3r_2 n(r_2) V_{dd}(|\vec{r}_1 - \vec{r}_2|)$$
$$= \underbrace{\left(\frac{N}{\pi^{3/2}R_\perp^2 R_z}\right)^2 \frac{C_{dd}}{8\pi}}_{S}\int d^3r_1 e^{-\frac{1}{R_\perp^2}[Ax_1^2+y_1^2+Bz_1^2+2Cx_1z_1]}$$
$$\times\int d^3r_2 e^{-\frac{1}{R_\perp^2}[Ax_2^2+y_2^2+Bz_2^2+2Cx_2z_2]}$$
$$\times\frac{(x_2-x_1)^2+(y_2-y_1)^2-2(z_2-z_1)^2}{[(x_2-x_1)^2+(y_2-y_1)^2+(z_2-z_1)^2]^{5/2}}, \tag{4.21}$$

next, shifting the coordinates, such as $x_2 - x_1 = x_3$, $y_2 - y_1 = y_3$, $z_2 - z_1 = z_3$, we write the energy as following

$$E_2^{int} = S\int d^3r_3 \frac{x_3^2+y_3^2-2z_3^2}{[x_3^2+y_3^2+z_3^2]^{5/2}} e^{-\frac{1}{R_\perp^2}[Ax_3^2+y_3^2+Bz_3^2+2Cx_3z_3]} \times I(x_1,y_1,z_1) \tag{4.22}$$

where

$$I(x_1,y_1,z_1) = I(y_1)\times I(x_1,z_1)$$

$$= \int dy_1 e^{-\frac{2}{R_\perp^2}[y_1^2+y_1y_3]}$$
$$\times\int dx_1 e^{-\frac{2}{R_\perp^2}[Ax_1^2+x_1(Ax_3+Cz_3)]}\int dz_1 e^{-\frac{2}{R_\perp^2}[Bz_1^2+z_1(Bz_3+Cx_3+2Cx_1)]}, \tag{4.23}$$

evaluating the integrals we end up with

$$I = \underbrace{\frac{\pi^{3/2}R_\perp^3}{\sqrt{8AB-2C^2}}}_{K} e^{y_3^2/2R_\perp^2} e^{\frac{1}{R_\perp^2}\left[\frac{(2AB-C^2)^2}{2B(4AB-C^2)}+\frac{C^2}{2B}\right]x_3^2}$$
$$\times e^{\frac{1}{R_\perp^2}\left[\frac{BC^2}{2(4AB-C^2)}+\frac{B}{2}\right]z_3^2}$$
$$\times e^{\frac{1}{R_\perp^2}\left[\frac{C(2AB-C^2)}{(4AB-C^2)}+C\right]x_3z_3}, \tag{4.24}$$

substitution of Eq. (4.24) back into Eq. (4.22) with changing of variables $x = x_3/R_\perp$, $y = y_3/R_\perp$, $z = z_3/R_\perp$ yields the following expression for the long-range interaction energy

$$E_2^{int} = SK\underbrace{\int d^3r \frac{x^2+y^2-2z^2}{[x^2+y^2+z^2]^{5/2}} e^{-a^2x^2/2-y^2/2-b^2z^2/2-d^2xz/2}}_{I(\alpha,\beta)} \tag{4.25}$$

with

$$a=\sqrt{\frac{4A(AB-C^2)}{4AB-C^2}},\qquad b=\sqrt{\frac{2B(2AB-C^2)}{4AB-C^2}},\qquad d=\sqrt{\frac{4ABC}{4AB-C^2}}$$

$$S=\left(\frac{N}{\pi^{3/2}R_\perp^2R_z}\right)^2\frac{C_{dd}}{8\pi},\qquad K=\frac{\pi^{3/2}R_\perp^3}{\sqrt{8AB-2C^2}}. \tag{4.26}$$

Having calculated the integral form of the interaction energy, as the next step, we make use of the Fourier transforms of the functions $\tilde{f}_1(\vec{k})$ and $\tilde{f}_2(\vec{k})$

$$f_1(\vec{r})=\frac{x^2+y^2-2z^2}{[x^2+y^2+z^2]^{5/2}},\qquad f_2(\vec{r})=e^{-a^2x^2/2-y^2/2-b^2z^2/2-d^2xz/2}, \tag{4.27}$$

to deal with the integral $I(\alpha,\beta)$. The Fourier transform $\tilde{f}_1(\vec{k})$ is given in Eq. (3.25) and we calculate $\tilde{f}_2(\vec{k})$ to be (appendix D)

$$\tilde{f}_2(\vec{k})=\frac{(2\pi)^{3/2}}{\sqrt{a^2b^2-d^4/4}}e^{-1/2k_y^2-\kappa^2k_x^2-\nu^2k_z^2-\mu^2k_xk_z} \tag{4.28}$$

where

$$\kappa=\sqrt{\frac{4b^2}{8a^2b^4-2b^2d^4}},$$

$$\nu=\sqrt{\frac{d^4}{8a^2b^4-2b^2d^4}+\frac{1}{2b^2}},$$

$$\mu=\sqrt{\frac{4b^2d^2}{2b^2d^4-8a^2b^4}}. \tag{4.29}$$

The long-range interaction energy with the Fourier transforms reads

$$\begin{aligned}E_2^{int}&=SK\int\frac{d^3k}{(2\pi)^3}\tilde{f}_1(\vec{k})\tilde{f}_2(\vec{k})\\&=SK\frac{4\pi}{(2\pi)^{3/2}}\frac{1}{\sqrt{a^2b^2-d^4/4}}\int d^3k\left(\frac{k_z^2}{k^2}-\frac{1}{3}\right)e^{-1/2k_y^2-\kappa^2k_x^2-\nu^2k_z^2-\mu^2k_xk_z}.\end{aligned} \tag{4.30}$$

To eliminate the cross term that appears in the exponential in Eq. (4.30), we carry out an arbitrary rotation around k_y axis, which is characterized by an angle χ such that

$$\begin{aligned} k'_z &= (\cos\chi)k_z + (\sin\chi)k_x \\ k'_x &= (\cos\chi)k_x - (\sin\chi)k_z \end{aligned} \tag{4.31}$$

the power of the exponential term that only includes k_x and k_z related terms then reads

$$\begin{aligned} -\kappa^2 k_x^2 - \nu^2 k_z^2 - \mu^2 k_x k_z =& (-\kappa^2\cos^2\chi - \nu^2\sin^2\chi + \mu^2\cos\chi\sin\chi)k_x'^2 \\ &+ (-\kappa^2\sin^2\chi - \nu^2\cos^2\chi - \mu^2\sin\chi\cos\chi)k_z'^2 \\ &+ \underbrace{[-\kappa^2 2\sin\chi\cos\chi + \nu^2 2\sin\chi\cos\chi - \mu^2(\cos^2\chi - \sin^2\chi)]}_{=0} k'_x k'_z \end{aligned}$$

where we equalized the term in square brackets to zero to get rid of the cross term, which generates the condition

$$(\nu^2 - \kappa^2)\sin 2\chi - \mu^2\cos 2\chi = 0 \implies \qquad \tan 2\chi = \frac{\mu^2}{\nu^2 - \kappa^2} \tag{4.32}$$

$$\sin 2\chi = \frac{\mu^2}{\sqrt{\mu^4 + (\nu^2 - \kappa^2)^2}}, \qquad \cos 2\chi = \frac{\nu^2 - \kappa^2}{\sqrt{\mu^4 + (\nu^2 - \kappa^2)^2}}, \tag{4.33}$$

and from the half angle formulas we have

$$\cos\chi = \left(\frac{\nu^2 - \kappa^2}{2\sqrt{\mu^4 + (\nu^2 - \kappa^2)^2}} + \frac{1}{2}\right)^{1/2}, \quad \sin\chi = \left(\frac{1}{2} - \frac{\nu^2 - \kappa^2}{2\sqrt{\mu^4 + (\nu^2 - \kappa^2)^2}}\right)^{1/2}. \tag{4.34}$$

then the energy in Eq. (4.30) becomes

$$E_2^{int} = SK\frac{4\pi}{(2\pi)^{3/2}}\frac{1}{\sqrt{a^2b^2 - d^4/4}}\int d^3k' \left[\frac{(k'_z\cos\chi - k'_x\sin\chi)^2}{k'^2} - \frac{1}{3}\right] e^{-1/2k_y'^2 - \epsilon^2 k_x'^2 - \eta^2 k_z'^2}$$

$$\begin{aligned} = SK\frac{4\pi}{(2\pi)^{3/2}}\frac{1}{\sqrt{a^2b^2 - d^4/4}}\Bigg[& \cos^2\chi \int d^3k' \frac{k_z'^2}{k'^2} e^{-1/2k_y'^2 - \epsilon^2 k_x'^2 - \eta^2 k_z'^2} \\ & + \sin^2\chi \int d^3k' \frac{k_x'^2}{k'^2} e^{-1/2k_y'^2 - \epsilon^2 k_x'^2 - \eta^2 k_z'^2} \\ & - 2\sin\chi\cos\chi \int d^3k' \frac{k'_x k'_z}{k'^2} e^{-1/2k_y'^2 - \epsilon^2 k_x'^2 - \eta^2 k_z'^2} \\ & - \int d^3k' \frac{1}{3} e^{-1/2k_y'^2 - \epsilon^2 k_x'^2 - \eta^2 k_z'^2} \Bigg] \end{aligned} \tag{4.35}$$

and the constants that newly appear

$$\epsilon = +\kappa^2 \cos^2\chi + \nu^2 \sin^2\chi - \mu^2 \sin\chi\cos\chi$$
$$\eta = +\kappa^2 \sin^2\chi + \nu^2 \cos^2\chi + \mu^2 \sin\chi\cos\chi. \tag{4.36}$$

As an initial attempt to solve the (or simplify) the integrals in Eq.(4.35), we take advantage of spherical coordinates

$$k'_x = k'\sin\theta\cos\phi \qquad k'_y = k'\sin\theta\sin\phi \qquad k'_z = k'\cos\theta, \tag{4.37}$$

and substitution of Eq.(4.37) into the Eq. (4.35) produces

$$\begin{aligned} E_2^{int} = SK\frac{4\pi}{(2\pi)^{3/2}}\frac{1}{\sqrt{a^2b^2 - d^4/4}} \\ \times\Bigg[\cos^2\chi\int_0^{2\pi}d\phi\int_0^{\pi}d(\cos\theta)\cos^2\theta\int_0^{\infty}dk'k'^2 e^{-k'^2\left[1/2\sin^2\theta\sin^2\phi - \epsilon^2\sin^2\cos^2\phi - \eta^2\cos^2\theta\right]} \\ + \sin^2\chi\int_0^{2\pi}d\phi\cos^2\phi\int_0^{\pi}d(\cos\theta)\cos^2\theta\int_0^{\infty}dk'k'^2 e^{-k'^2\left[1/2\sin^2\theta\sin^2\phi - \epsilon^2\sin^2\cos^2\phi - \eta^2\cos^2\theta\right]} \\ - \frac{\sqrt{2}\pi^{3/2}}{3\epsilon\eta}\Bigg], \end{aligned} \tag{4.38}$$

where we used the fact that the integral proportional to $\sin\chi\cos\chi$ has zero contribution and the last integral in Eq. (4.35) which is trivial to solve and the result is directly written. Performing the Gaussian integrals corresponding to k' integral and making a change of variable $x = \cos\theta$ we get

$$\begin{aligned} E_2^{int} = SK\frac{4\pi}{(2\pi)^{3/2}}\frac{1}{\sqrt{a^2b^2 - d^4/4}}\frac{\sqrt{\pi}}{4} \\ \times\Bigg[\cos^2\chi\int_0^{2\pi}d\phi\int_{-1}^{1}dx\frac{x^2}{\left[(1/2\sin^2\phi + \epsilon^2\cos^2\phi)(1-x^2) + \eta^2x^2\right]^{3/2}} \\ + \sin^2\chi\int_0^{2\pi}d\phi\cos^2\phi\int_{-1}^{1}dx\frac{1-x^2}{\left[(1/2\sin^2\phi + \epsilon^2\cos^2\phi)(1-x^2) + \eta^2x^2\right]^{3/2}} \\ - \frac{4\sqrt{2}\pi}{3\epsilon\eta}\Bigg] \\ = SK \times I(\alpha,\beta). \end{aligned} \tag{4.39}$$

The long-range interaction energy displayed in Eq. (4.39) is in the simplest form that we write for numerical calculation (θ integral is analytically solvable

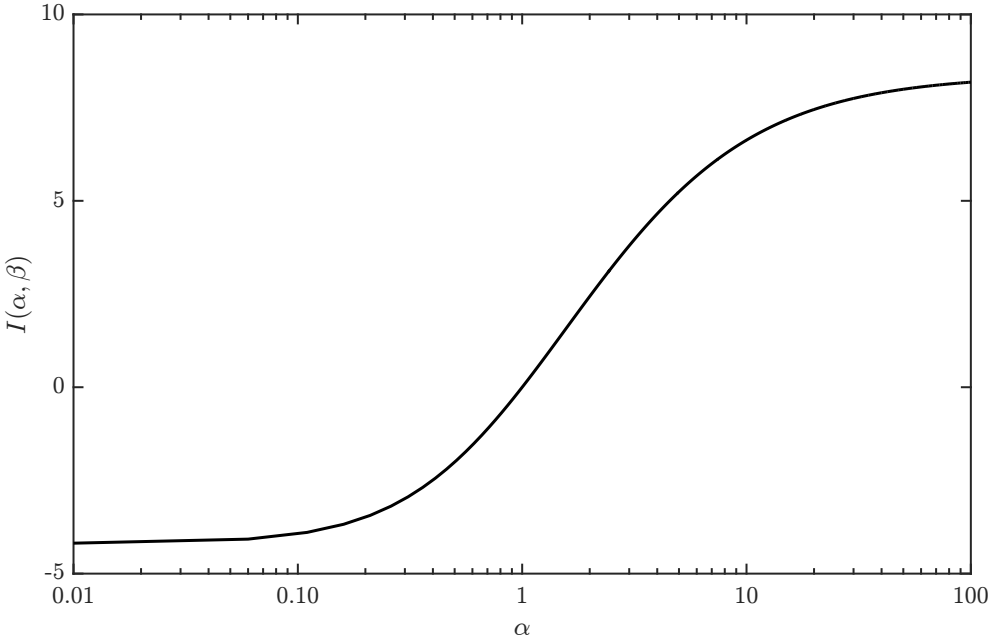

Figure 4.3: The Integral $I(\alpha, \beta)$ simplifies to the integral $I(\alpha)$ in Eq. (3.31) when $\gamma = \beta = 0$ (plot of the latter integral can be visualized as the multiplication of $f(\alpha)$ plot in Fig 3.3 by a factor of $-4\pi/3$) showing that our manipulation of the integrals are correct.

but 2D numerical solution gives faster results and this way, we also prevent new constants from appearing). From this point on, we will numerically calculate the integrals in Eq. (4.39) and check the validity of the numerical results by comparing them to the limit of the previous problem (chapter 3), namely when $\gamma = \beta = 0$ (Fig. 4.3).

4.2 Dimensionless Total Energy

The energy of the system is put into dimensionless form by using the same scaling parameters described in Sec. 3.2. The total dimensionless energy

$$\tilde{E}(\tilde{R}_\perp, \tilde{R}_z, \beta) = \frac{E}{N\hbar\bar{\omega}} = \tilde{E}_{kin} + \tilde{E}_{pot} + \tilde{E}_1^{int} + \tilde{E}_2^{int} \tag{4.40}$$

of the system reads from the equations (4.8), (4.15), (4.18), (4.39) and subject to the scaling parameters (3.34),

$$\tilde{E} = \frac{1}{4}\left(\frac{2}{\tilde{R}_\perp^2}+\frac{1}{\tilde{R}_z^2}\right)+\frac{1}{4\lambda^{2/3}}\left[\tilde{R}_\perp^2+(\cos^2\beta+\lambda^2\sin^2\beta)\tilde{R}_\perp^2+(\sin^2\beta+\lambda^2\cos^2\beta)\tilde{R}_z^2\right] + \frac{\tilde{g}}{4\sqrt{2}\pi^{3/2}\tilde{R}_\perp^2\tilde{R}_z}+\frac{3}{\pi^{3/2}(8\pi)\sqrt{8AB-2C^2}}\frac{\tilde{g}}{\tilde{R}_\perp\tilde{R}_z^2}\epsilon_{dd}\times I(\alpha,\beta). \tag{4.41}$$

with

$$\begin{aligned} I(\alpha,\beta) =& \frac{4\pi}{(2\pi)^{3/2}}\frac{1}{\sqrt{a^2b^2-d^4/4}}\frac{\sqrt{\pi}}{4} \\ &\times\left[\cos^2\chi\int_0^{2\pi}d\phi\int_{-1}^{1}dx\frac{x^2}{\left[(1/2\sin^2\phi+\epsilon^2\cos^2\phi)(1-x^2)+\eta^2x^2\right]^{3/2}}\right. \\ &+\sin^2\chi\int_0^{2\pi}d\phi\cos^2\phi\int_{-1}^{1}dx\frac{1-x^2}{\left[(1/2\sin^2\phi+\epsilon^2\cos^2\phi)(1-x^2)+\eta^2x^2\right]^{3/2}} \\ &\left.-\frac{4\sqrt{2}\pi}{3\epsilon\eta}\right]. \end{aligned} \tag{4.42}$$

Minimized form of the energy (4.41) for parameters $R_\perp$, R_z and β describes the new elongation direction of the condensate by means of the minimum value β_{min} and the equilibrium radii $R_{\perp,min}$, $R_{z,min}$ of the condensate along radial and z directions (with respect to primed coordinates), respectively. This energy also portrays the stability dynamics depending on the strength and nature (attractive or repulsive) of the interparticle interactions (contact and dipolar) and geometry of the system. Thus far, we have locally emphasized that in the limit of $\gamma=\beta=0$, integral $I(\alpha,\beta)$ and the potential energy simplifies to their counterparts in chapter 3. This statement is also valid for the total energy in Eq. (4.41), and it is easy to check that in this limit $A=1$, $B=\alpha^2$, $C=0$ and the total energy is identical to the one presented in Eq. (3.38).

In the Thomas-Fermi limit, energy in Eq. (4.41) can be written as a function

of the condensate aspect ratio α and the radius of the condensate along z, R_z,

$$\tilde{E}(\alpha,\tilde{R}_z,\beta) = \frac{\tilde{R}_z^2}{4\lambda^{2/3}}\left[\alpha^2+(\cos^2\beta+\lambda^2\sin^2\beta)\alpha^2+(\sin^2\beta+\lambda^2\cos^2\beta)\right] + \frac{\tilde{g}}{4\sqrt{2}\pi^{3/2}\alpha^2\tilde{R}_z^3}+\frac{3}{\pi^{3/2}(8\pi)\sqrt{8AB-2C^2}}\frac{\tilde{g}}{\alpha\tilde{R}_z^3}\epsilon_{dd}\times I(\alpha,\beta). \tag{4.43}$$

4.3 Geometrical Stabilization

The two crucial factors that determine the elongation direction of the condensate, are the dipolar interaction (and its strength with respect to the contact interaction) between constituent particles of the condensate and the external trapping potential as depicted in Fig. 4.1. Particulary, it is foreseen that the strength of the dipole-dipole interaction (specified by ϵ_{dd}) and the alignment direction of dipoles; aspect ratio λ of the trap should be the defining factors in the final stable configuration of the condensate. The logic is that, elongation of the condensate is expected to occur along z' direction which is specified by the angle β, however for a strong dipolar interaction the angle β should be more and more close to the dipole angle γ and when the strength of the interaction is strong enough, the two angles could be even the same. A similar discussion can be made from the trap side: for a constant power of the dipolar interaction, as the trap aspect ratio increases from extremely cigar-shaped trap ($\lambda = 0.1$) to almost spherical trap ($\lambda = 0.99$), the angle β should increase from zero to γ. Consequently, competition between the strength of the dipolar interaction with dipoles oriented along z'' and the sphericity of the confining trap will determine the ultimate shape of the condensate.

We have minimized the the energy (4.41) for different orientation angles γ of dipoles. Our calculation for the optimal values of the variational parameters $R_{\perp,min}$, $R_{z,min}$ and β_{min} ($0 \leq \beta_{min} \leq \gamma$) shows that, the final shape of the condensate is commonly determined by the trap aspect ratio λ and the relative strength of dipolar and contact interactions ϵ_{dd}, as we have expected. In the limiting case of nearly spherical trap with trap aspect ratio $\lambda = 0.99$ and for $\epsilon_{dd} =$

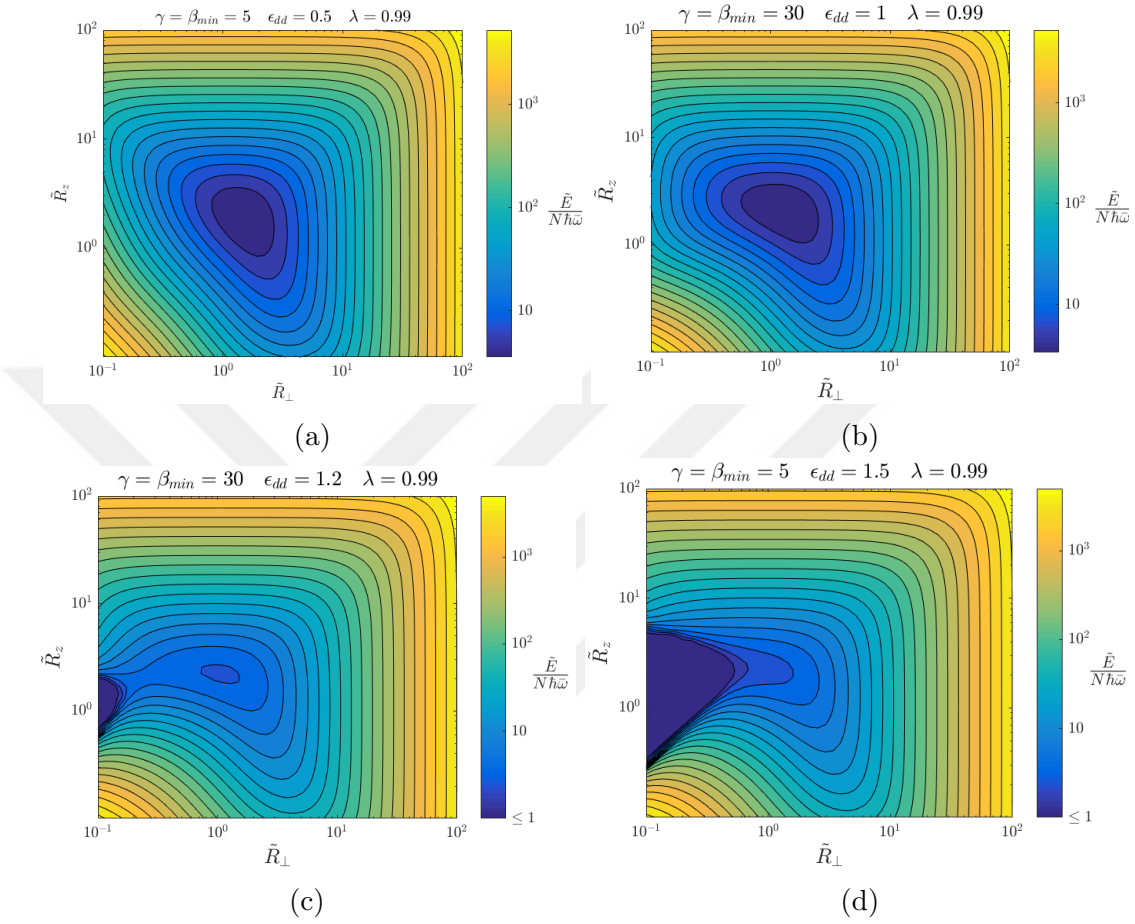

Figure 4.4: Contour plots of the dimensionless energy $\tilde{E}(\tilde{R}_\perp, \tilde{R}_z, \beta)$ in Eq. (4.41) in the spherical limit of the trap, for fixed values of $\tilde{g} = 180$ and $\lambda = 0.99$; for different values of the parameter ϵ_{dd} as shown on the figures.

0.5, we have observed that the condensate elongates along the same direction as the orientation of dipoles, namely $\beta_{min} = \gamma$ (Fig. 4.5a) with a global minimum of the energy in the energy landscape (Fig. 4.4a). The fact that γ is the maximum angle that the condensate could elongate along encourages us to examine the stability of the condensate in the spherical limit of the trap, to achieve that we gradually increase the value of $\epsilon_{dd} = 1,\ 1.2,\ 1.5$ while keeping λ constant at 0.99. The energy landscape of the condensate has a global minimum for the values $0 \leq \epsilon_{dd} \leq 1$ meaning a stable state (e.g. Fig. 4.4b), whereas for values started to be increased from unity, it switches to a metastable state with local minimum and saddle points (Fig 4.4c), and increasing even further results in the disappearance of the local minimum and the condensate is in a collapsed unstable

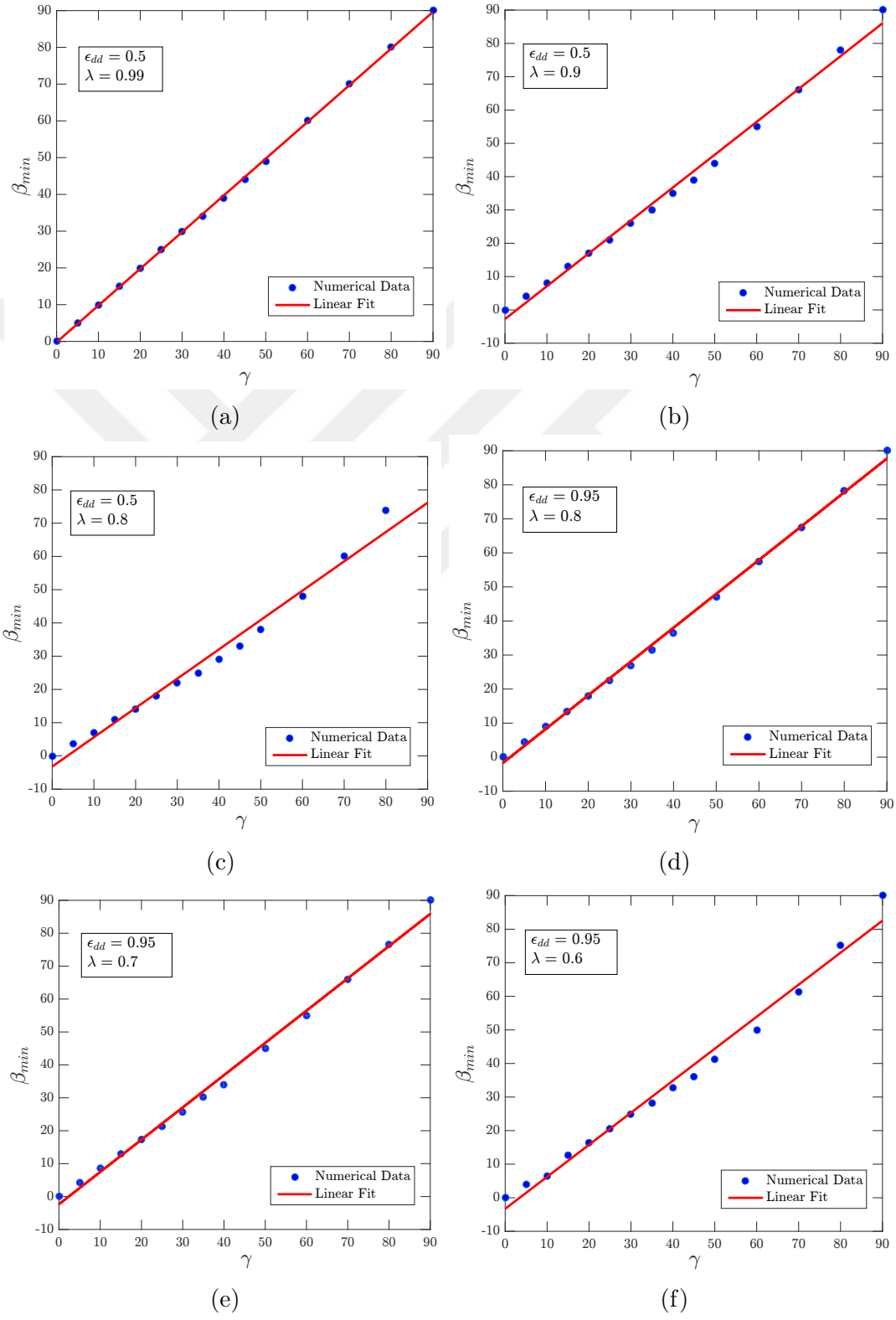

Figure 4.5: The dipole orientation angle γ versus condensate elongation angle β graphs for pair of the parameters ϵ_{dd}, λ and corresponding values are shown on the figures.

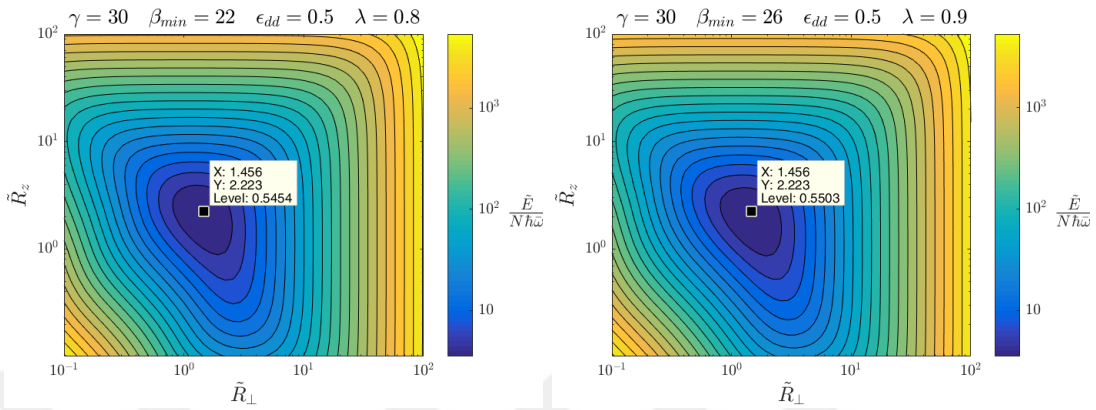

(a) (b)

Figure 4.6: Contour plots of the dimensionless energy $\tilde{E}(\tilde{R}_\perp, \tilde{R}_z, \beta)$ for the two cases (a) $\gamma = 30$, $\epsilon_{dd} = 0.5$, $\lambda = 0.9$; (b) $\gamma = 30$, $\epsilon_{dd} = 0.5$, $\lambda = 0.8$.

state (Fig. 4.4d). It could also be observed by comparing Fig. 4.4a and Fig 4.4b that angle of the dipole orientation γ , in spherical limit for the trap, does not affect the stability of the condensate, consequently angle values we write on the top of the contour plots are irrelevant as long as we take the two angles to be the same. In addition to the comparison of the figures, increasing ϵ_{dd} intrinsically causes an enhancement in the elongation in the same direction as the $R_{\perp,min}$ decreases and $R_{z,min}$ increases.

Having investigated the limiting case which enabled us to examine the stability condition of the condensate depending on the relative strengths of the interparticle interactions (contact and dipolar), we next study how the elongation of the condensate will be affected when we increase the prolateness of the trap by decreasing the trap aspect ratio (from $\lambda = 0.99$) λ and keeping the ϵ_{dd} constant (Fig. 4.5). We infer from our manipulations that, as the trap aspect ratio decreases, the condensate elongation direction z' approaches to the trap symmetry axis z while the angle β decreases for the same initial orientation γ of the dipoles. Similarly, decreasing ϵ_{dd} while keeping the trap aspect ratio constant has exactly the same effect. As a third case, increasing ϵ_{dd} at constant λ results in an elongation direction getting closer to the orientation direction z'' of dipoles as in the case of spherical limit of the trap. Therefore, we may safely state that given the

initial direction of the external field, the elongation direction is entirely determined by the overall contributions of the dipolar interaction (compared to the contact interaction) and the trapping potential, confirming our initial guesses. It is also worth pointing out that, as can be inferred from the Fig. 4.5, γ and β has a linear relation and the slope of the corresponding line decrease with decreasing λ. In addition, comparison of the figures 4.4a, 4.6a and 4.6b depicts that, although elongation direction is changing with decreasing (or increasing) trap aspect ratio, the optimal values of the radii ($R_{\perp,min}$ and $R_{z,min}$) are not, meaning that the condensate is preserving its elongated shape (with $R_{\perp,min} < R_{z,min}$) during the change of direction.

Consequently, we have created a new geometry accommodating the features of a dipolar interaction that we have described in the chapters so far. We have seen that, readjusting the direction of the external field have provided us with a flexible geometry through which we could control the elongation direction of the condensate with the essential stability conditions are unchanged. The stable, metastable and unstable states of the condensate are investigated in the limit of a spherical trap.

Chapter 5

Conclusion

In a BEC, we have thus far emphasized how the effects of the interparticle interactions can introduce a new set of properties to the system. In particular, geometry dependent stabilization of dBEC has been investigated in chapters 3 and 4 with a Gaussian trial function. We have observed that despite the simplicity that the Gaussian density profile introduced to the calculations, the integrals we encountered or the process of minimization for the purpose of determining final configuration of the condensate, were far from being trivial in the both of the problems dealt with.

A better but formidable approximation of the discussion made in chapter 4 could be done by invoking a Thomas-Fermi ansatz as described in Sec. 3.5. However, we should stress that in the case of the same directions for the trap symmetry and the orientation of the dipoles, both of the trial functions results in the same transcendental equation which gives the relation between condensate and trap aspect ratios. This shows that utilization of the Gaussian density profile is not a poor approximation for the sake of variational procedure and estimating the stability of the condensate. We are curious about the fact that whether this will be the case for the problem of separate directions with calculations made by using Thomas-Fermi anzats.

The new geometry we have suggested is to be improved by both considering nonequal radii (i.e. $R_x \neq R_y$) with Gaussian trial function and Thomas-Fermi trial functions, respectively. Possible additions maybe taking into account the particular values of the parameters that are used in the experiments or corresponding to the specific species such as chromium, dysprosium and erbium to explore their stability dynamics.

Bibliography

[1] S. Bose, "Plancks law and light quantum hypothesis," *Z. Phys*, vol. 26, p. 178, 1924.

[2] A. Einstein, "Quantentheorie des einatomigen idealen gases," *Sitzungsber. Kgl. Preuss. Akad. Wiss.*, 1924.

[3] A. Einstein, "Quantentheorie des einatomigen idealen gases. zweite abhandlung (quantum theory of monatomic ideal gases, part two)," *Sitzungsber. Kgl. Preuss. Akad. Wiss.*, vol. 1, no. 3, 1925.

[4] P. Kapitza, "Viscosity of liquid helium below the λ-point," *Nature*, vol. 141, no. 3558, p. 74, 1938.

[5] J. Allen and A. Misener, "Flow phenomena in liquid helium II," *Nature*, vol. 142, no. 3597, pp. 643–644, 1938.

[6] F. London, "The λ-Phenomenon of liquid helium and the Bose-Einstein degeneracy," *Nature*, vol. 141, p. 643, 1938.

[7] M. H. Anderson, J. R. Ensher, M. R. Matthews, C. E. Wieman, and E. A. Cornell, "Observation of Bose-Einstein condensation in a dilute atomic vapor," *Science*, vol. 269, no. 5221, pp. 198–201, 1995.

[8] K. B. Davis, M. O. Mewes, M. R. Andrews, N. J. van Druten, D. S. Durfee, D. M. Kurn, and W. Ketterle, "Bose-Einstein condensation in a gas of sodium atoms," *Phys. Rev. Lett.*, vol. 75, pp. 3969–3973, Nov 1995.

[9] C. C. Bradley, C. A. Sackett, J. J. Tollett, and R. G. Hulet, "Evidence of Bose-Einstein condensation in an atomic gas with attractive interactions," *Phys. Rev. Lett.*, vol. 75, pp. 1687–1690, Aug 1995.

[10] J. Weiner, V. S. Bagnato, S. Zilio, and P. S. Julienne, "Experiments and theory in cold and ultracold collisions," *Rev. Mod. Phys.*, vol. 71, pp. 1–85, Jan 1999.

[11] D. G. Fried, T. C. Killian, L. Willmann, D. Landhuis, S. C. Moss, D. Kleppner, and T. J. Greytak, "Bose-Einstein condensation of atomic hydrogen," *Phys. Rev. Lett.*, vol. 81, pp. 3811–3814, Nov 1998.

[12] G. Modugno, G. Ferrari, G. Roati, R. J. Brecha, A. Simoni, and M. Inguscio, "Bose-Einstein condensation of potassium atoms by sympathetic cooling," *Science*, vol. 294, no. 5545, pp. 1320–1322, 2001.

[13] A. Robert, O. Sirjean, A. Browaeys, J. Poupard, S. Nowak, D. Boiron, C. I. Westbrook, and A. Aspect, "A Bose-Einstein condensate of metastable atoms," *Science*, vol. 292, no. 5516, pp. 461–464, 2001.

[14] T. Weber, J. Herbig, M. Mark, H.-C. Nägerl, and R. Grimm, "Bose-Einstein condensation of cesium," *Science*, 2002.

[15] Y. Takasu, K. Maki, K. Komori, T. Takano, K. Honda, M. Kumakura, T. Yabuzaki, and Y. Takahashi, "Spin-singlet Bose-Einstein condensation of two-electron atoms," *Phys. Rev. Lett.*, vol. 91, p. 040404, Jul 2003.

[16] S. Stellmer, M. K. Tey, B. Huang, R. Grimm, and F. Schreck, "Bose-Einstein condensation of strontium," *Phys. Rev. Lett.*, vol. 103, p. 200401, Nov 2009.

[17] Y. N. M. de Escobar, P. G. Mickelson, M. Yan, B. J. DeSalvo, S. B. Nagel, and T. C. Killian, "Bose-Einstein condensation of ^{84}Sr," *Phys. Rev. Lett.*, vol. 103, p. 200402, Nov 2009.

[18] S. Kraft, F. Vogt, O. Appel, F. Riehle, and U. Sterr, "Bose-Einstein condensation of alkaline earth atoms: ^{40}Ca," *Phys. Rev. Lett.*, vol. 103, p. 130401, Sep 2009.

[19] S. Jochim, M. Bartenstein, A. Altmeyer, G. Hendl, S. Riedl, C. Chin, J. Hecker Denschlag, and R. Grimm, "Bose-Einstein condensation of molecules," *Science*, vol. 302, no. 5653, pp. 2101–2103, 2003.

[20] M. W. Zwierlein, C. A. Stan, C. H. Schunck, S. M. F. Raupach, S. Gupta, Z. Hadzibabic, and W. Ketterle, "Observation of Bose-Einstein condensation of molecules," *Phys. Rev. Lett.*, vol. 91, p. 250401, Dec 2003.

[21] C. A. Regal, M. Greiner, and D. S. Jin, "Observation of resonance condensation of fermionic atom pairs," *Phys. Rev. Lett.*, vol. 92, p. 040403, Jan 2004.

[22] Doyle, J., Friedrich, B., Krems, R. V., and Masnou-Seeuws, F., "Editorial: Quo vadis, cold molecules?," *Eur. Phys. J. D*, vol. 31, no. 2, pp. 149–164, 2004.

[23] A. Griesmaier, J. Werner, S. Hensler, J. Stuhler, and T. Pfau, "Bose-Einstein condensation of chromium," *Phys. Rev. Lett.*, vol. 94, p. 160401, Apr 2005.

[24] Q. Beaufils, R. Chicireanu, T. Zanon, B. Laburthe-Tolra, E. Maréchal, L. Vernac, J.-C. Keller, and O. Gorceix, "All-optical production of chromium Bose-Einstein condensates," *Phys. Rev. A*, vol. 77, p. 061601, Jun 2008.

[25] S. Giovanazzi, A. Görlitz, and T. Pfau, "Tuning the dipolar interaction in quantum gases," *Phys. Rev. Lett.*, vol. 89, p. 130401, Sep 2002.

[26] K. Aikawa, A. Frisch, M. Mark, S. Baier, A. Rietzler, R. Grimm, and F. Ferlaino, "Bose-Einstein condensation of erbium," *Phys. Rev. Lett.*, vol. 108, p. 210401, May 2012.

[27] M. Lu, N. Q. Burdick, S. H. Youn, and B. L. Lev, "Strongly dipolar Bose-Einstein condensate of dysprosium," *Phys. Rev. Lett.*, vol. 107, p. 190401, Oct 2011.

[28] M. Fattori, G. Roati, B. Deissler, C. D'Errico, M. Zaccanti, M. Jona-Lasinio, L. Santos, M. Inguscio, and G. Modugno, "Magnetic dipolar interaction in a Bose-Einstein condensate atomic interferometer," *Phys. Rev. Lett.*, vol. 101, p. 190405, Nov 2008.

[29] S. E. Pollack, D. Dries, M. Junker, Y. P. Chen, T. A. Corcovilos, and R. G. Hulet, "Extreme tunability of interactions in a ^{7}Li Bose-Einstein condensate," *Phys. Rev. Lett.*, vol. 102, p. 090402, Mar 2009.

[30] K.-K. Ni, S. Ospelkaus, M. De Miranda, A. Pe'er, B. Neyenhuis, J. Zirbel, S. Kotochigova, P. Julienne, D. Jin, and J. Ye, "A high phase-space-density gas of polar molecules," *Science*, vol. 322, no. 5899, pp. 231–235, 2008.

[31] C.-H. Wu, J. W. Park, P. Ahmadi, S. Will, and M. W. Zwierlein, "Ultracold fermionic feshbach molecules of ^{23}Na^{40}K," *Phys. Rev. Lett.*, vol. 109, p. 085301, Aug 2012.

[32] J. W. Park, S. A. Will, and M. W. Zwierlein, "Ultracold dipolar gas of fermionic ^{23}Na^{40}K molecules in their absolute ground state," *Phys. Rev. Lett.*, vol. 114, p. 205302, May 2015.

[33] V. Bendkowsky, B. Butscher, J. Nipper, J. P. Shaffer, R. Löw, and T. Pfau, "Observation of ultralong-range Rydberg molecules," *Nature*, vol. 458, no. 7241, pp. 1005–1008, 2009.

[34] J. R. Anglin and W. Ketterle, "Bose-Einstein condensation of atomic gases," *Nature*, vol. 416, no. 6877, pp. 211–218, 2002.

[35] M. Weidemüller and C. Zimmermann, "Interactions in ultracold gases: from atoms to molecules," *Wiley-VCH*, 2003.

[36] S. Yi and L. You, "Trapped atomic condensates with anisotropic interactions," *Phys. Rev. A*, vol. 61, p. 041604, Mar 2000.

[37] K. Góral, K. Rzążewski, and T. Pfau, "Bose-Einstein condensation with magnetic dipole-dipole forces," *Phys. Rev. A*, vol. 61, p. 051601, Mar 2000.

[38] D. O'Dell, S. Giovanazzi, G. Kurizki, and V. M. Akulin, "Bose-Einstein condensates with $1/r$ interatomic attraction: Electromagnetically induced "gravity"," *Phys. Rev. Lett.*, vol. 84, pp. 5687–5690, Jun 2000.

[39] L. Santos, G. V. Shlyapnikov, P. Zoller, and M. Lewenstein, "Bose-Einstein condensation in trapped dipolar gases," *Phys. Rev. Lett.*, vol. 85, pp. 1791–1794, Aug 2000.

[40] S. Giovanazzi, D. O'Dell, and G. Kurizki, "Self-binding transition in Bose condensates with laser-induced "gravitation"," *Phys. Rev. A*, vol. 63, p. 031603, Feb 2001.

[41] J.-P. Martikainen, M. Mackie, and K.-A. Suominen, "Comment on "Bose-Einstein condensation with magnetic dipole-dipole forces"," *Phys. Rev. A*, vol. 64, p. 037601, Aug 2001.

[42] D. DeMille, "Quantum computation with trapped polar molecules," *Phys. Rev. Lett.*, vol. 88, p. 067901, Jan 2002.

[43] S. Giovanazzi, D. O'Dell, and G. Kurizki, "Density modulations of Bose-Einstein condensates via laser-induced interactions," *Phys. Rev. Lett.*, vol. 88, p. 130402, Mar 2002.

[44] K. Góral, L. Santos, and M. Lewenstein, "Quantum phases of dipolar bosons in optical lattices," *Phys. Rev. Lett.*, vol. 88, p. 170406, Apr 2002.

[45] M. Baranov, L. Dobrek, K. Gral, L. Santos, and M. Lewenstein, "Ultracold dipolar gases – a challenge for experiments and theory," *Physica Scripta*, vol. 2002, no. T102, p. 74, 2002.

[46] L. Santos, G. V. Shlyapnikov, and M. Lewenstein, "Roton-maxon spectrum and stability of trapped dipolar Bose-Einstein condensates," *Phys. Rev. Lett.*, vol. 90, p. 250403, Jun 2003.

[47] F. Deuretzbacher, J. C. Cremon, and S. M. Reimann, "Ground-state properties of few dipolar bosons in a quasi-one-dimensional harmonic trap," *Phys. Rev. A*, vol. 81, p. 063616, Jun 2010.

[48] D. H. J. O'Dell, S. Giovanazzi, and C. Eberlein, "Exact hydrodynamics of a trapped dipolar Bose-Einstein condensate," *Phys. Rev. Lett.*, vol. 92, p. 250401, Jun 2004.

[49] J. Stuhler, A. Griesmaier, T. Koch, M. Fattori, T. Pfau, S. Giovanazzi, P. Pedri, and L. Santos, "Observation of dipole-dipole interaction in a degenerate quantum gas," *Phys. Rev. Lett.*, vol. 95, p. 150406, Oct 2005.

[50] R. M. W. van Bijnen, D. H. J. O'Dell, N. G. Parker, and A. M. Martin, "Dynamical instability of a rotating dipolar Bose-Einstein condensate," *Phys. Rev. Lett.*, vol. 98, p. 150401, Apr 2007.

[51] D. H. J. O'Dell and C. Eberlein, "Vortex in a trapped Bose-Einstein condensate with dipole-dipole interactions," *Phys. Rev. A*, vol. 75, p. 013604, Jan 2007.

[52] C. Ticknor, R. M. Wilson, and J. L. Bohn, "Anisotropic superfluidity in a dipolar Bose gas," *Phys. Rev. Lett.*, vol. 106, p. 065301, Feb 2011.

[53] F. Dalfovo, S. Giorgini, L. P. Pitaevskii, and S. Stringari, "Theory of Bose-Einstein condensation in trapped gases," *Rev. Mod. Phys.*, vol. 71, pp. 463–512, Apr 1999.

[54] J. O. Andersen, "Theory of the weakly interacting Bose gas," *Rev. Mod. Phys.*, vol. 76, pp. 599–639, Jul 2004.

[55] C. J. Pethick and H. Smith, *Bose-Einstein Condensation in Dilute Gases*. Cambridge University Press, second ed., 2008. Cambridge Books Online.

[56] L. P. Pitaevskii and S. Stringari, *Bose-Einstein condensation*. No. 116, Oxford University Press, 2003.

[57] A. Griffin, D. W. Snoke, and S. Stringari, *Bose-Einstein condensation*. Cambridge University Press, 1996.

[58] C. Eberlein, S. Giovanazzi, and D. H. J. O'Dell, "Exact solution of the Thomas-Fermi equation for a trapped Bose-Einstein condensate with dipole-dipole interactions," *Phys. Rev. A*, vol. 71, p. 033618, Mar 2005.

[59] T. Lahaye, C. Menotti, L. Santos, M. Lewenstein, and T. Pfau, "The physics of dipolar bosonic quantum gases," *Reports on Progress in Physics*, vol. 72, no. 12, p. 126401, 2009.

[60] N. G. Parker and D. H. J. O'Dell, "Thomas-Fermi versus one- and two-dimensional regimes of a trapped dipolar Bose-Einstein condensate," *Phys. Rev. A*, vol. 78, p. 041601, Oct 2008.

[61] S. Yi and L. You, "Trapped condensates of atoms with dipole interactions," *Phys. Rev. A*, vol. 63, p. 053607, Apr 2001.

[62] C. P. Frahm, "Some novel delta-function identities," *American Journal of Physics*, vol. 51, no. 9, pp. 826–829, 1983.

Appendix A

Integral appearing in the Fourier transform calculation of the long-range energy term

We shall begin with setting $a = (\alpha^2 - 1)/\alpha^2$, and attempt to evaluate the following integral

$$I_{E_2^{int}} = \int_{-1}^{1} dx \frac{x^2 - \frac{1}{3}}{(1 - a^2 x^2)^{3/2}}$$

$$= \int_{-1}^{1} dx \frac{x^2}{(1 - a^2 x^2)^{3/2}} - \frac{1}{3} \int_{-1}^{1} dx \frac{1}{(1 - a^2 x^2)^{3/2}}. \tag{A.1}$$

making the following change of variaables: $x = 1/a \sin u \Rightarrow dx = 1/a \cos u du$, $u = \arcsin(ax)$ we get

$$I_{E_2^{int}} = \frac{1}{a^3} \int_{-\arcsin(a)}^{\arcsin(a)} du \frac{\sin^2 u}{\cos^2 u} - \frac{1}{3a} \int_{-\arcsin(a)}^{\arcsin(a)} du \frac{1}{\cos^2 u}$$

$$= \frac{1}{a^3} \int_{-\arcsin(a)}^{\arcsin(a)} du \tan^2 u - \frac{1}{3a} \int_{-\arcsin(a)}^{\arcsin(a)} du \sec^2 u, \tag{A.2}$$

where $\tan^2 u = \sec^2 u - 1$ and $\int \sec^2 u = \tan u + \text{const.}$, we have

$$\begin{aligned} I_{E_2^{int}} &= \left[\frac{1}{a^3}(\tan u - u) - \frac{1}{3a} \tan u \right]_{-\arcsin(a)}^{\arcsin(a)} \\ &= \left[\frac{3-a^2}{3a^2} \tan u - \frac{u}{a^3} \right]_{-\arcsin(a)}^{\arcsin(a)} \\ &= \frac{3-a^2}{3a^3} \left[\tan(\arcsin a) - \tan(-\arcsin a) \right] - \frac{2}{a^3} \arcsin(a) \\ &= \frac{3-a^2}{3a^3} \left(\frac{2a}{\sqrt{1-a^2}} \right) - \frac{2}{a^3} \arctan\left(\frac{a}{\sqrt{1-a^2}} \right) \\ &= \frac{6-2a^2}{3a^2\sqrt{1-a^2}} - \frac{2}{a^3} \arctan\left(\frac{a}{\sqrt{1-a^2}} \right) \end{aligned} \tag{A.3}$$

Substituting back for a yields the following terms

$$\circ \ \frac{6-2a^2}{3a^2\sqrt{1-a^2}} = \frac{2}{3}\alpha \frac{1+2\alpha^2}{\alpha^2-1}, \tag{A.4}$$

$$\circ \ \frac{2}{a^3} = -\frac{2\alpha^3}{i(1-\alpha^2)^{3/2}}, \tag{A.5}$$

$$\circ \ \frac{a}{\sqrt{1-a^2}} = i\sqrt{1-\alpha^2}, \tag{A.6}$$

and inserting these terms into (A.3) with $\arctan(i\sqrt{1-\alpha^2}) = i \operatorname{arctanh}(\sqrt{1-\alpha^2})$,

$$\begin{aligned} I_{E_2^{int}} &= -\frac{2}{3}\alpha \frac{1+2\alpha^2}{1-\alpha^2} + \frac{2\alpha^3}{i(1-\alpha^2)^{3/2}} \arctan(i\sqrt{1-\alpha^2}) \\ &= -\frac{2}{3}\alpha \left[\frac{1+2\alpha^2}{1-\alpha^2} - \frac{3\alpha^2}{(1-\alpha^2)^{3/2}} \operatorname{arctanh}(\sqrt{1-\alpha^2}) \right]. \end{aligned} \tag{A.7}$$

Appendix B

Derivation of the Transcendental Equation

The minimization condition $d\tilde{E}(\alpha)/d\alpha = 0$ for the energy (3.43) yields the following equality:

$$\begin{aligned}
&\frac{d}{d\alpha}\left\{\frac{(2\alpha^2+\lambda^2)^{3/5}}{\alpha^{4/5}}\left[1-\epsilon_{dd}f(\alpha)\right]^{2/5}\right\} \\
&\quad = \left[1-\epsilon_{dd}f(\alpha)\right]^{2/5}\frac{d}{d\alpha}\left[\frac{(2\alpha^2+\lambda^2)^{3/5}}{\alpha^{4/5}}\right] \\
&\quad + \frac{(2\alpha^2+\lambda^2)^{3/5}}{\alpha^{4/5}}\frac{d}{d\alpha}\left\{\left[1-\epsilon_{dd}f(\alpha)\right]^{2/5}\right\} = 0
\end{aligned} \tag{B.1}$$

with derivatives

$$\circ\ \frac{d}{d\alpha}\frac{(2\alpha^2+\lambda^2)^{3/5}}{\alpha^{4/5}} = \frac{4(\alpha^2-\lambda^2)}{5\alpha^{9/5}(2\alpha^2\lambda^2)^{2/5}}, \tag{B.2}$$

$$\circ\ \frac{d}{d\alpha}\left[1-\epsilon_{dd}f(\alpha)\right]^{2/5} = \frac{-\frac{2}{5}\epsilon_{dd}\frac{d}{d\alpha}f(\alpha)}{\left[1-\epsilon_{dd}f(\alpha)\right]^{3/5}}, \tag{B.3}$$

$$\circ\ \frac{d}{d\alpha}f(\alpha) = -\frac{2}{\alpha} + \left[\frac{3\alpha}{1-\alpha^2}+\frac{2}{\alpha}\right]f(\alpha). \tag{B.4}$$

Substituting derivatives in (B.2), (B.4), (B.4) into the Eq. (B.1) and multiplying resulting expression by $5\alpha^{4/5}(2\alpha^2+\lambda^2)[1-\epsilon_{dd}f(\alpha)]^{3/5}/2$, we get the Eq.(3.44).

Appendix C

Dipolar Meanfield Potential in Spherical Symmetry

In this section we demonstrate the steps of calculation of the integral (3.54). The function ϕ is defined in Sec. 3.5 to be

$$\phi(r) = \int d^3r' \frac{n(\vec{r'})}{|\vec{r} - \vec{r'}|} \tag{C.1}$$

and $n(r)$ is the TF density given in Eq. (3.53), therefore Eq. (C.1) reads

$$\phi(r) = \frac{1}{4\pi} \frac{m\omega_0^2 R^2}{2g} \int_0^{2\pi} d\phi \int_0^{\pi} d\theta \sin\theta \int_0^{R} dr' \frac{1 - r'^2/R^2}{\sqrt{r^2 + r'^2 - 2\vec{r} \cdot \vec{r'}}} \tag{C.2}$$

setting $r = z$ (spherical symmetry) we have

$$\phi(r) = \frac{2\pi}{4\pi} \frac{m\omega_0^2 R^2}{2g} \int_0^{R} dr' \int_0^{\pi} d\theta \frac{1 - r'^2/R^2}{\sqrt{z^2 + r'^2 - 2zr' \cos\theta}} \sin\theta \tag{C.3}$$

setting

$$\begin{aligned} y &= z + r'^2 - 2zr' \cos\theta \\ dy &= 2zr' \sin\theta d\theta \end{aligned} \tag{C.4}$$

Then,

$$\phi(r) = \frac{m\omega_0^2 R^2}{4g} \int_0^R dr' \int_{(z-r')^2}^{(z+r')^2} dy \frac{(1 - r'^2/R^2)/2z}{\sqrt{y}}$$

$$= \frac{m\omega_0^2 R^2}{4gz} \int_0^R dr' r' \left(1 - \frac{r'^2}{R^2}\right) \sqrt{y}\Big|_{(z-r')^2}^{(z+r')^2}$$

$$= \frac{m\omega_0^2 R^2}{4gr} \int_0^R dr' r' \left(1 - \frac{r'^2}{R^2}\right) [r + r' - |r - r'|] \,. \tag{C.5}$$

We make use of the Eq. (C.5) in Sec. 3.6 to find the dipolar potential inside and outside regions of the condensate.

Appendix D

Fourier Transform of the Rotated Density

The part of the Gaussian density (4.19) that is subject to Fourier transform is the function we defined as $f_2(\vec{r})$ in Eq. (4.27). For completeness, we depict the calculating steps of its Fourier transform $\tilde{f}_2(\vec{k})$. s

$$\begin{aligned}\tilde{f}_2(-\vec{k}) &= \int_{-\infty}^{\infty} f_2(\vec{r}) e^{i\vec{k}\cdot\vec{r}} \\ &= \int_{-\infty}^{\infty} dy e^{ik_y - y^2/2} \int_{-\infty}^{\infty} dx e^{ik_x - a^2x^2/2} \int_{-\infty}^{\infty} e^{ik_z - b^2z^2/2 - d^2xz/2} \\ &= \int_{-\infty}^{\infty} dy e^{-k_y^2/2} e^{-1/2(y-ik_y)^2} \int_{-\infty}^{\infty} dx e^{ik_x - a^2x^2/2} \int_{-\infty}^{\infty} dz e^{(ik_z - d^2x/2)z - b^2z^2/2}\end{aligned} \tag{D.1}$$

letting $y' = y - ik_y$, $z' = zb$,

$$\begin{aligned}\tilde{f}_2(-\vec{k}) &= e^{-k_y^2/2} \int_{-\infty}^{\infty} dy e^{-y'^2 - 2} \int_{-\infty}^{\infty} dx e^{ik_x - a^2x^2/2} \int_{-\infty}^{\infty} \frac{dz'}{b} e^{(ik_z - d^2x/2)z'/b - z'^2/2} \\ &= \sqrt{2\pi} e^{-k_y^2/2} \int_{-\infty}^{\infty} dx e^{ik_x x - a^2x^2/2 + 1/2b^2(ik_z - d^2x/2)^2} \int_{-\infty}^{\infty} \frac{dz'}{b} e^{-1/2[z' - 1/b(ik_z - d^2x/2)]^2}\end{aligned} \tag{D.2}$$

making the change of variable $z'' = [z' - 1/b(ik_z - d^2x/2)]$ we have,

$$\begin{aligned}
\tilde{f}_2(-\vec{k}) &= \frac{\sqrt{2\pi}}{b} e^{-k_y^2/2} \int_{-\infty}^{\infty} dx e^{ik_x x - a^2x^2/2 + 1/2b^2(ik_z - d^2x/2)^2} \underbrace{\int_{-\infty}^{\infty} dz'' e^{-z''^2/2}}_{\sqrt{2\pi}} \\
&= \frac{\sqrt{2\pi}}{b} e^{-k_y^2/2} \int_{-\infty}^{\infty} dx e^{-(a^2 - d^4/4b^2)x^2/2 + (ik_x - ik_z d^2/2b^2)x - k_z^2/2b^2} \\
&= \frac{(2\pi)^{3/2}}{b} e^{-k_y^2/2 - k_z^2/2b^2} \frac{1}{\sqrt{a^2 - d^4/4b^2}} e^{(2ik_x b^2 - ik_z d^2)^2/8b^4(a^2 - d^4/4b^2)} \\
&= \frac{(2\pi)^{3/2}}{\sqrt{a^2b^2 - d^4/4}} e^{-k_y^2/2 - k_z^2/2b^2} e^{-(4b^4k_x^2 - 4b^2d^2k_xk_z + d^4k_z^2)/(8a^2b^4 - 2b^2d^4)} \\
&\quad . \qquad \text{(D.3)}
\end{aligned}$$

Final form of the transform is the following expression,

$$\begin{aligned}
\tilde{f}_2(-\vec{k}) = \frac{(2\pi)^{3/2}}{\sqrt{a^2b^2 - d^4/4}} & e^{-k_y^2/2} \\
& \times e^{-[4b^4/(8a^2b^4 - 2b^2d^4)]k_x^2} \\
& \times e^{-[d^4/(8a^2b^4 - 2b^2d^4) + 1/2b^2]k_z^2} \\
& \times e^{-[4b^2d^2/(2b^2d^4 - 8a^2b^4)]k_xk_z}, \qquad \text{(D.4)}
\end{aligned}$$

where the dimensionless parameters a, b and d are given in Eq. (4.26). The expression (D.4) immediately simplifies to the Eq. (3.27) in the limit $\gamma = \beta = 0$, i.e. when there is no rotation of cartesian coordinates (Fig. 4.1).